LETTER

doi:10.1038/nature14264

AAV-expressed eCD4-Ig provides durable protection from multiple SHIV challenges

Matthew R. Gardner[1]*, Lisa M. Kattenhorn[2]*, Hema R. Kondur[1], Markus von Schaewen[3], Tatyana Dorfman[1], Jessica J. Chiang[2], Kevin G. Haworth[4], Julie M. Decker[5], Michael D. Alpert[2,6], Charles C. Bailey[1], Ernest S. Neale Jr[2], Christoph H. Fellinger[1], Vinita R. Joshi[1], Sebastian P. Fuchs[7], Jose M. Martinez-Navio[7], Brian D. Quinlan[1], Annie Y. Yao[2], Hugo Mouquet[8,9], Jason Gorman[10], Baoshan Zhang[10], Pascal Poignard[11], Michel C. Nussenzweig[8,12], Dennis R. Burton[11,13], Peter D. Kwong[10], Michael Piatak Jr[14], Jeffrey D. Lifson[14], Guangping Gao[15], Ronald C. Desrosiers[2,7], David T. Evans[16], Beatrice H. Hahn[5], Alexander Ploss[3], Paula M. Cannon[4], Michael S. Seaman[17] & Michael Farzan[1]

Long-term *in vivo* expression of a broad and potent entry inhibitor could circumvent the need for a conventional vaccine for HIV-1. Adeno-associated virus (AAV) vectors can stably express HIV-1 broadly neutralizing antibodies (bNAbs)[1,2]. However, even the best bNAbs neutralize 10–50% of HIV-1 isolates inefficiently (80% inhibitory concentration (IC_{80}) > 5 μg ml^{-1}), suggesting that high concentrations of these antibodies would be necessary to achieve general protection[3–6]. Here we show that eCD4-Ig, a fusion of CD4-Ig with a small CCR5-mimetic sulfopeptide, binds avidly and cooperatively to the HIV-1 envelope glycoprotein (Env) and is more potent than the best bNAbs (geometric mean half-maximum inhibitory concentration (IC_{50}) < 0.05 μg ml^{-1}). Because eCD4-Ig binds only conserved regions of Env, it is also much broader than any bNAb. For example, eCD4-Ig efficiently neutralized 100% of a diverse panel of neutralization-resistant HIV-1, HIV-2 and simian immunodeficiency virus isolates, including a comprehensive set of isolates resistant to the CD4-binding site bNAbs VRC01, NIH45-46 and 3BNC117. Rhesus macaques inoculated with an AAV vector stably expressed 17–77 μg ml^{-1} of fully functional rhesus eCD4-Ig for more than 40 weeks, and these macaques were protected from several infectious challenges with SHIV-AD8. Rhesus eCD4-Ig was also markedly less immunogenic than rhesus forms of four well-characterized bNAbs. Our data suggest that AAV-delivered eCD4-Ig can function like an effective HIV-1 vaccine.

Rhesus macaques inoculated with an AAV-based gene-therapy vector express antibody-like immunoadhesins for years, and these immunoadhesins afforded partial protection from a neutralization-sensitive simian immunodeficiency virus (SIV)[2], suggesting that long-term sterilizing protection from HIV-1 might be achievable without a conventional vaccine. Full-length AAV-expressed bNAbs also protected humanized mice from an HIV-1 challenge[1,7]. However, a large fraction of HIV-1 isolates remain partially or wholly resistant to even the best bNAbs, with IC_{80} values greater than 5 μg ml^{-1} measured under optimal *in vitro* conditions[3–6] (Extended Data Table 1). Higher concentrations will probably be necessary for broad-based protection *in vivo*, but primate studies suggest that these concentrations will be difficult to establish in humans[2,8]. An effective AAV-based vaccine may therefore require broader and more potent inhibitors of HIV-1 entry.

The breadth of an antibody depends on the conservation of its epitope. The two most conserved epitopes of HIV-1 Env are its CD4- and coreceptor-binding sites[9–11]. The immunoadhesin form of CD4, CD4-Ig, has been extensively studied as a therapeutic. It neutralizes most isolates, irreversibly inactivates Env, and is demonstrated safe for use in humans[12–15]. However, its affinity for Env is lower than those of bNAbs[16], and its potency is further compromised by its parallel ability to promote infection[17]. Mimetics of the primary HIV-1 coreceptor CCR5, in particular peptides based on its tyrosine-sulfated amino terminus, have also been characterized[18,19]. These sulfopeptides bind Env specifically but with low affinity in the absence of CD4, in part because they include hydrophobic residues and *O*-linked glycosylation that impede their association with Env[18,20]. CCR5mim1, a 15-amino-acid sulfopeptide derived from the HIV-1 neutralizing antibody E51 (ref. 21), lacks these interfering elements (Fig. 1a) and binds Env with higher affinity than CCR5-based peptides[20,22]. Reflecting the conservation of the sulfotyrosine-binding pockets of Env[9,10], CCR5mim1 binds both CCR5- and CXCR4-dependent Env proteins from all HIV-1 clades[20,22].

We reasoned that a fusion of CD4-Ig and CCR5mim1 would bind Env cooperatively and with higher avidity than either molecule alone. Accordingly, three fusion proteins were generated (sequences in Extended Data Fig. 1). CCR5mim1 was inserted at either the CD4-Ig amino terminus (fusion 1), between the CD4 and Fc domain (fusion 2), or at the CD4-Ig carboxy terminus (fusion 3, renamed eCD4-Ig). All three CD4-Ig variants neutralized CCR5- and CXCR4-dependent isolates more efficiently than did CD4-Ig, with eCD4-Ig consistently the most potent (Extended Data Fig. 2a, b). eCD4-Ig neutralized a wider panel of HIV-1 isolates and SIVmac316 with 10- to 100-fold lower IC_{50} values than CD4-Ig (Fig. 1b). Improved neutralization of SIVmac316 is consistent with conservation of the sulfotyrosine-binding pockets of Env[9,10], and a first indication of the exceptional breadth of eCD4-Ig.

To understand better the markedly greater potency of eCD4-Ig relative to CD4-Ig, we compared their abilities to bind cell-surface-expressed Env trimers (Fig. 1c). At low concentrations, eCD4-Ig bound these trimers more efficiently than did CD4-Ig. Surprisingly, eCD4-Ig saturated trimer-expressing cells with approximately one-third less bound protein than CD4-Ig, suggesting that the sulfopeptides of eCD4-Ig made some CD4-binding sites inaccessible. eCD4-Ig also less efficiently promoted HIV-1 infection of CCR5-positive, CD4-negative cells than CD4-Ig (Fig. 1d), presumably because its sulfopeptides blocked virion access to cell-surface CCR5. Heterodimers of CD4-Ig and eCD4-Ig[23]

[1]Department of Infectious Diseases, The Scripps Research Institute, Jupiter, Florida 33458, USA. [2]Department of Comparative Pathology, Harvard Medical School, New England Primate Research Center, Southborough, Massachusetts 01772, USA. [3]Department of Molecular Biology, Princeton University, Princeton, New Jersey 08544, USA. [4]Department of Molecular Microbiology and Immunology, Keck School of Medicine of the University of Southern California, Los Angeles, California 90033, USA. [5]Departments of Medicine and Microbiology, Perelman School of Medicine, University of Pennsylvania, Philadelphia, Pennsylvania 19104, USA. [6]Immunathon Inc., Cambridge, Massachusetts 02141, USA. [7]Department of Pathology, University of Miami Miller School of Medicine, Miami, Florida 33136, USA. [8]Laboratory of Molecular Immunology, The Rockefeller University, New York, New York 10065, USA. [9]Department of Immunology, Institut Pasteur, Paris, 75015, France. [10]Vaccine Research Center, National Institutes of Health, Bethesda, Maryland 20892, USA. [11]Department of Immunology and Microbial Science, IAVI Neutralizing Antibody Center, and Center for HIV/AIDS Vaccine Immunology and Immunogen Discovery, The Scripps Research Institute, La Jolla, California 92037, USA. [12]Howard Hughes Medical Institute, New York, New York 10065, USA. [13]Ragon Institute of MGH, MIT and Harvard, Cambridge, Massachusetts 02139, USA. [14]AIDS and Cancer Virus Program, Leidos Biomedical Research, Incorporated, Frederick National Laboratory for Cancer Research, Frederick, Maryland 21702, USA. [15]Gene Therapy Center, University of Massachusetts Medical School, Worcester, Massachusetts 01655, USA. [16]Department of Pathology and Laboratory Medicine, University of Wisconsin, Madison, Wisconsin 53711, USA. [17]Beth Israel Deaconess Medical Center, Boston, Massachusetts 02215, USA.

*These authors contributed equally to this work.

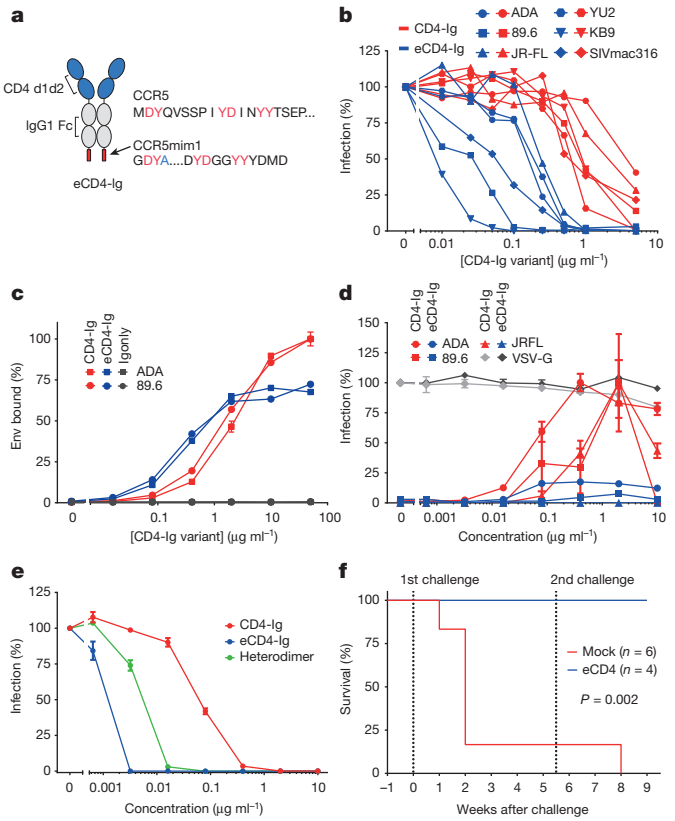

Figure 1 | Functional characterization of eCD4-Ig. a, CD4-Ig is comprised of CD4 domains 1 and 2 (blue) fused to the human IgG1 Fc domain (grey). In eCD4-Ig, the sulfopeptide CCR5mim1 (red) is fused to the C terminus of CD4-Ig. The sequence of the CCR5 N terminus is provided for comparison. Common residues, including four CCR5 sulfotyrosines, are shown in red. CCR5mim1 Ala 4 (blue) is substituted with Tyr in CCR5mim2, described below. **b**, HIV-1 pseudotyped with the Env proteins of the indicated HIV-1 or SIV isolates was incubated with GHOST-CCR5 cells and varying concentrations of CD4-Ig (red) or eCD4-Ig (blue). Infection was measured as green fluorescent protein (GFP)-expression by flow cytometry. Errors of replicates are less than 20% of indicated values but not indicated for clarity. **c**, 293T cells transfected to express 89.6 or ADA Env proteins were incubated with the indicated concentrations of CD4-Ig (red), eCD4-Ig (blue) or IgG (grey) and analysed by flow cytometry. **d**, HIV-1 expressing luciferase and pseudotyped with the Env proteins of the indicated isolates was incubated with Cf2Th-CCR5 cells in the presence of varying concentrations of CD4-Ig (red) or eCD4-Ig (blue). Experiment was controlled with HIV-1 pseudotyped with the VSV-G protein (grey). Infection normalized to the maximum value observed for each pseudovirus. **e**, HIV-1 pseudotyped with the 89.6 Env was incubated with TZM-bl cells and varying concentration of CD4-Ig (red), eCD4-Ig (blue) or a CD4-Ig/eCD4-Ig heterodimer (green). Similar experiments using additional Env proteins are shown in Extended Data Fig. 2c, d. **f**, Infection curves of humanized NSG mice with 2–4 μg ml^{-1} of serum eCD4-Ig at time of HIV-1_{NL4-3} challenges (blue line, $n = 5$), or mock treated (red line, $n = 6$) are shown. Three uninfected eCD4-Ig treated mice and the sole uninfected mock treated mouse were rechallenged 5 weeks after the first challenge. Significant protection ($P = 0.002$; Mantel–Cox test) was observed in the eCD4-Ig-treated group. Viral load measurements are shown in Extended Data Fig. 2h. Experiments in **b**–**e** were performed at least twice with each indicated isolate with similar results. Errors bars denote one s.e.m. of duplicates.

neutralized less potently than eCD4-Ig (Fig. 1e and Extended Data Fig. 2c–e), indicating that both eCD4-Ig sulfopeptides engage the Env trimer, consistent with a model of eCD4-Ig bound to Env (Extended Data Fig. 3) and previous studies of CCR5mim1 (ref. 24). Thus, the markedly greater potency of eCD4-Ig relative to CD4-Ig is due in part to the higher avidity with which it binds Env and to its decreased ability to promote infection.

We next assessed eCD4-Ig under more physiological conditions. We observed that eCD4-Ig, but not CD4-Ig, halted replication of infectious viruses in human peripheral blood mononuclear cells (PBMC) at concentrations as low as 125 ng ml^{-1} (Extended Data Fig. 1f, g). We administered sufficient eCD4-Ig to humanized NOD/SCID/*Il2rg*$^{-/-}$ (NSG) mice to maintain serum concentrations of 2–4 μg ml^{-1} at the time of challenge. Five eCD4-Ig-treated mice and six control mice were challenged intravenously with 5×10^4 infectious units of HIV-1_{NL4-3}. Five out of six control mice, but no eCD4-Ig-inoculated mice, were infected (Fig. 1f and Extended Data Fig. 2h). Five weeks later, three eCD4-Ig-treated mice and the uninfected control mouse were rechallenged. Again, no eCD4-Ig-treated mouse was infected, whereas the control mouse became infected.

We then characterized the ability of eCD4-Ig to neutralize a diverse panel of neutralization-resistant tier 2 and 3 viruses[25] (Extended Data Figs 4a and 5a). In parallel, we assayed three additional eCD4-Ig variants. In the first, eCD4-Ig^{mim2}, CCR5mim1 was replaced by CCR5mim2, which differs from CCR5mim1 by a single Ala to Tyr substitution[22]. We also introduced a previously characterized Gln 40 to Ala mutation into the CD4 domain 1 of eCD4-Ig (eCD4-Ig^{Q40A})[16]. Both mutations were combined in a final variant (eCD4-Ig^{Q40A,mim2}). eCD4-Ig and these variants substantially outperformed CD4-Ig for every virus in the panel, typically improving neutralization potency by 20- to >200-fold. Underscoring its breadth, eCD4-Ig neutralized SIVmac251 33 times more efficiently than CD4-Ig. In general, the more neutralization-resistant a virus, the better eCD4-Ig and its variants performed relative to CD4-Ig. In most cases, replacement of CCR5mim1 with CCR5mim2 modestly improved neutralization. Similarly, the Gln40Ala mutation also improved neutralization of most HIV-1 isolates, but not of SIVmac251.

We compared eCD4-Ig, eCD4-Ig^{mim2} and eCD4-Ig^{Q40A,mim2} with a panel of 12 antibodies and inhibitors using three additional HIV-1 isolates (Fig. 2a and Extended Data Fig. 6a, b). eCD4-Ig and its variants neutralized the SG3 and YU2 isolates more efficiently than any of these inhibitors. Five bNAbs neutralized JR-CSF more efficiently than any eCD4-Ig variant, but four of these could not neutralize SG3. All eCD4-Ig variants neutralized these isolates with IC_{50} values less than 0.3 μg ml^{-1}, which is more efficiently than CD4-Ig, the tetrameric CD4-Ig variant PRO-542 (refs 12, 14), or the antibodies 2G12, 4E10 and VRC01. eCD4-Ig and its variants, but not three CD4-binding site bNAbs, neutralized the neutralization-resistant SIVmac239 as well as HIV-2 strain ST (Fig. 2b and Extended Data Fig. 6c). As observed with SIVmac251, the Gln40Ala variant was less efficient at neutralizing SIVmac239 and HIV-2. The potency of these eCD4-Ig variants was also reflected in their abilities to mediate antibody-dependent cell-mediated cytotoxicity (ADCC). eCD4-Ig, eCD4-Ig^{mim2} and eCD4-Ig^{Q40A,mim2} each facilitated 30–40 times more killing of infected cells by CD16$^+$ natural killer cells[26] than did CD4-Ig or the antibody IgGb12 (Fig. 2c). Thus the C-terminal modification of eCD4-Ig did not interfere with the ADCC effector function of its Fc domain.

We further evaluated eCD4-Ig, eCD4-Ig^{mim2}, eCD4-Ig^{Q40A,mim2} and the bNAb NIH45-46 using nearly every isolate reported to be resistant to either of the CD4bs antibodies NIH45-46 or 3BNC117 (Extended Data Figs 4b and 5b). Both eCD4-Ig variants efficiently neutralized all 38 resistant isolates assayed with IC_{50} values ranging from <0.001 to 1.453 μg ml^{-1}. By contrast, 26 isolates in this panel were confirmed to be resistant to NIH45-46. Previous reports found 29 and 18 isolates to be resistant to 3BCN117 and VRC01, respectively[4,6]. Figure 3 and Extended Data Fig. 7 summarize the neutralization studies compiled from the experiments in Figs 1 and 2 and Extended Data Figs 4–6, and from previous studies of VRC01 and 3BNC117 against the same isolates[4]. They show that the geometric mean IC_{50} and IC_{80} values of eCD4-Ig and its variants are less than 0.05 μg ml^{-1} (500 pM) and 0.2 μg ml^{-1} (2 nM), respectively, roughly 3–4 times lower than those of VRC01, NIH45-46 or 3BNC117. Importantly, our lead eCD4-Ig variant, eCD4-Ig^{mim2}, neutralized 100% of the isolates assayed at concentrations (IC_{50} < 1.5 μg ml^{-1}; IC_{80} < 5.2 μg ml^{-1}) that are probably sustainable in humans.

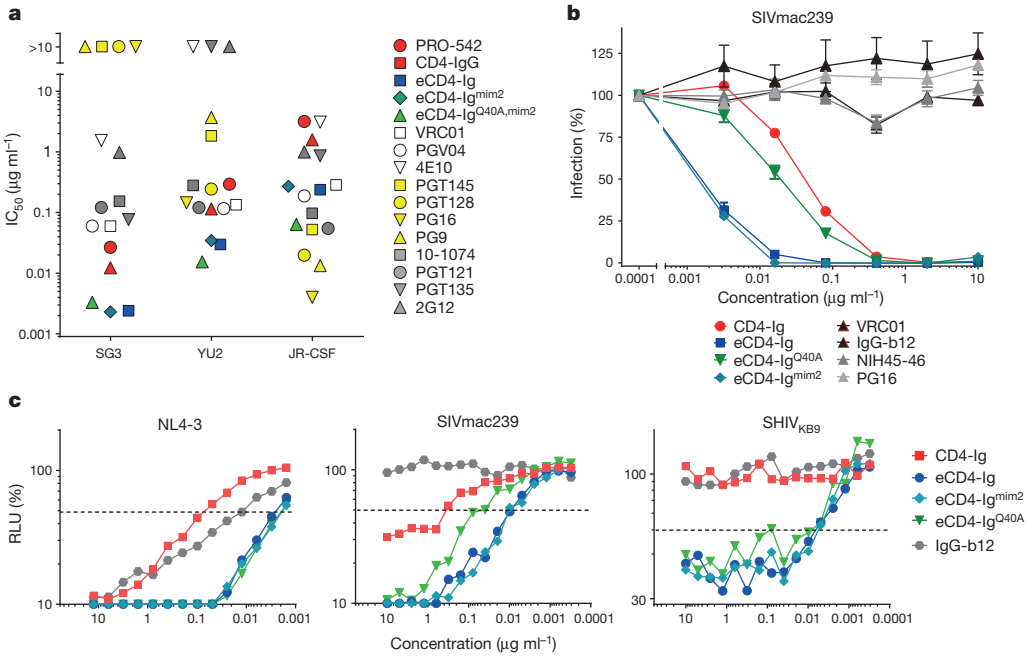

Figure 2 | Comparison of eCD4-Ig variants and HIV-1 neutralizing antibodies. **a**, HIV-1 pseudotyped with the Env proteins of the indicated isolates were incubated with TZM-bl cells and varying concentrations of the indicated entry inhibitors, and the resulting IC_{50} values are plotted. IC_{90} values and standard errors are presented in Extended Data Fig. 6a, b. **b**, Experiments similar to those in **a** except that HIV-1 pseudotyped with the SIVmac239 Env was incubated with varying concentrations of CD4-Ig, eCD4-Ig variants or CD4bs antibodies. Extended Data Fig. 6c shows a similar study using the HIV-2 ST Env. Errors bars denote one s.e.m. of triplicates. **c**, ADCC activity was assessed using CEM.NKR-CCR5 target cells incubated with infectious HIV-1 NL4-3, SIVmac239 or $SHIV_{KB9}$ for 4 days. Cells were then incubated with KHYG-1 NK effector cells[26] for 8 h in the presence of the indicated inhibitors. ADCC activity was measured as loss of luciferase activity from the target cells. RLU, relative light units. All experiments represented in this figure were performed at least twice with each isolate and inhibitor with similar results. Error bars indicate one s.e.m. of triplicates.

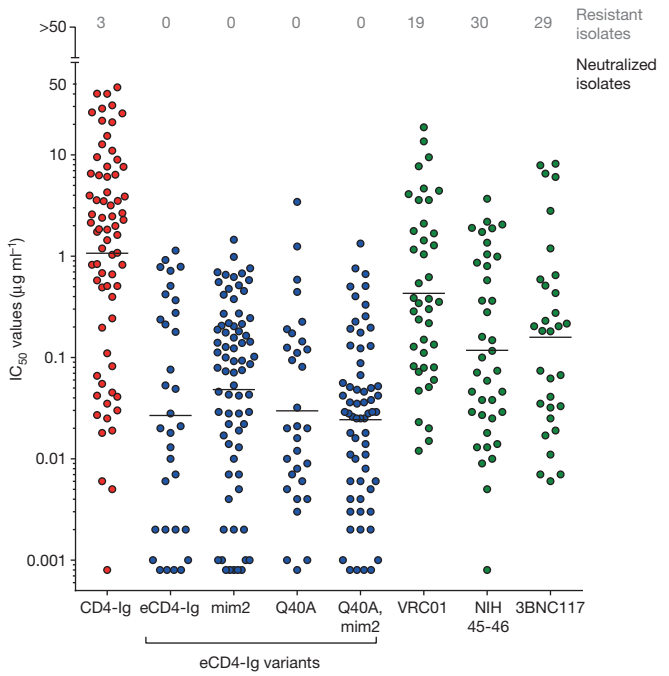

Figure 3 | Summary of HIV-1, HIV-2 and SIV neutralization studies. The IC_{50} values from studies of Figs 1b, 2a, b and Extended Data Figs 4–6 are plotted. The numbers of isolates resistant to 50 μg ml^{-1} of the indicated inhibitors are indicated at the top. Geometric means are calculated for neutralized isolates and indicated with horizontal lines. Note that these data include 38 HIV-1 isolates selected for resistance to NIH45-46 or 3BNC117, so that isolates resistant to these antibodies are over-represented. Nonetheless, the geometric mean values of neutralized viruses are consistent with previous reports (Extended Data Table 1). Data for VRC01 and 3BNC117 were reported previously[4,6]. IC_{80} values are presented in Extended Data Fig. 7.

Finally, using a rhesus macaque form of eCD4-Ig^{mim2}, we investigated whether AAV-delivered eCD4-Ig could function like an HIV-1 vaccine. To minimize potential adverse reactions, the Fc domain of rhesus IgG2, which binds Fc receptors and complement less efficiently than IgG1, was used. We also introduced an Ile39Asn mutation into the CD4 domain[27] to correct partially the lower affinity of rhesus CD4 for most HIV-1 isolates (Extended Data Fig. 8a, b). The gene for the resulting construct, rh-eCD4-IgG2^{I39N,mim2} (described hereafter as rh-eCD4-Ig), was cloned into a single-stranded AAV2 vector (AAV-rh-eCD4-Ig; Extended Data Fig. 8c). A total of 2.5×10^{13} AAV1-encapsidated particles delivering this vector were administered into the quadriceps of four four-year-old male Indian-origin rhesus macaques. To promote rh-eCD4-Ig sulfation, a separate single-stranded AAV vector expressing rhesus tyrosine-protein sulfotransferase 2 (AAV-rh-TPST2; Extended Data Fig. 8c) was co-administered with AAV-rh-eCD4-Ig at a 1:4 ratio. No adverse reactions were observed in any of the AAV-rh-eCD4-Ig-inoculated macaques. These macaques and four age- and gender-matched controls were challenged intravenously with increasing doses of SHIV-AD8 (Fig. 4a, b). Sixteen weeks after AAV inoculation, two control macaques became infected following challenge with 200 pg p27. A subsequent 400 pg challenge infected a third control animal, and, after resisting an additional 400 pg challenge, the final control was infected with 800 pg, 34 weeks from the date of AAV inoculation. None of these challenges infected AAV-rh-eCD4-Ig-inoculated macaques, indicating that eCD4-Ig protected them from four doses capable of infecting control animals.

Measured rh-eCD4-Ig titres in the serum stabilized to between 17 and 77 μg ml^{-1} over the last 10 weeks of the 40-week study period (Fig. 4c). Two macaques expressed less than 20 μg ml^{-1} at the time of the final 800 pg challenge, suggesting that this concentration could prevent many otherwise infectious exposures in humans. Sera from inoculated macaques neutralized HIV-1 as efficiently as laboratory-prepared rh-eCD4-Ig mixed with pre-inoculation sera (Fig. 4d and Extended Data Fig. 8d),

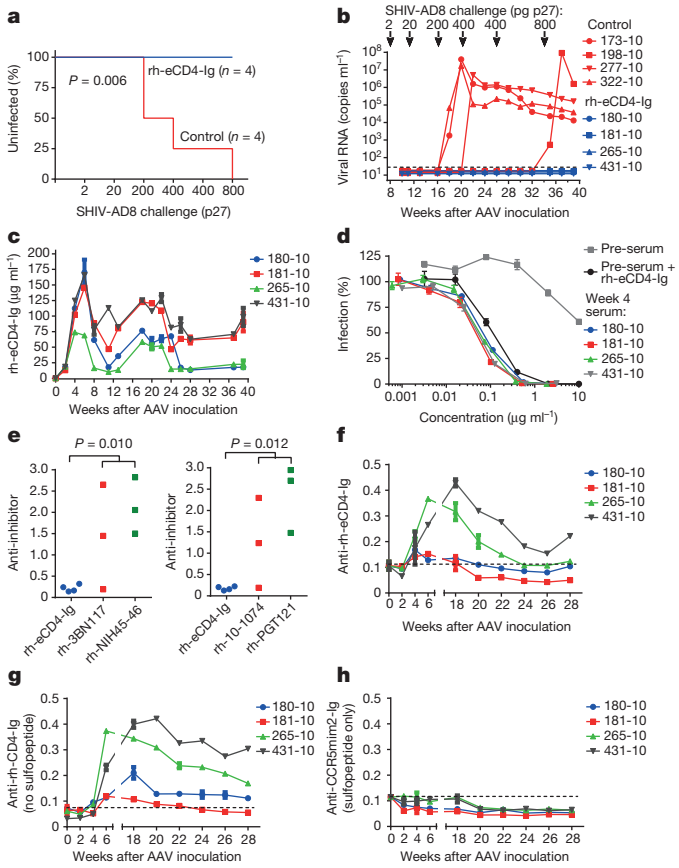

Figure 4 | AAV-rh-eCD4-Ig protects rhesus macaques from SHIV-AD8. **a**, Infection analysis comparing four male Indian-origin rhesus macaques inoculated intramuscularly with 2×10^{13} AAV particles delivering rh-eCD4-Ig (blue) and four age- and gender-matched controls (red). At 8, 11, 16, 20, 26 and 34 weeks after inoculation, macaques were challenged with the indicated p27 titres of SHIV-AD8. Significant protection ($P = 0.006$; Mantel–Cox test) was observed in the AAV-rh-eCD4-Ig-treated group. **b**, Viral loads of inoculated (blue) and control (red) macaques are shown, with the time and titre of challenge indicated above the graph. **c**, Concentrations of rh-eCD4-Ig in the sera of inoculated macaques were measured by ELISA to week 40 after inoculation. **d**, The neutralizing potency of macaque sera obtained 4 weeks after AAV-inoculation was compared to pre-inoculation sera (pre-sera), and pre-sera mixed with laboratory-produced rh-eCD4-Ig, as in Fig. 2b. **e**, Anti-transgene antibody responses in AAV-rh-eCD4-Ig-inoculated macaques were compared to those in macaques inoculated with AAV expressing the indicated bNAbs bearing constant regions of rhesus IgG2. Sera from 4 weeks after inoculation were analysed. Plates were coated with equivalent amounts of rh-eCD4-Ig or rhesus forms of bNAbs and incubated with sera and anti-rhesus lambda chain (left) or kappa chain (right) antibody conjugated to horseradish peroxidase. Note that 3BNC117 and NIH45-46 bear a kappa light chain, whereas PGT121 and 10-1074 bear a lambda light chain, so that only host antibody responses were detected. Values indicate absorbance at 450 nM. *P* values (Student's two-tailed *t*-test) are indicated above the figures. **f**, The sensitivity of the assay in **e** was increased to measure longitudinally the anti-rh-eCD4-Ig activity in the sera of inoculated macaques. Both anti-kappa and anti-lambda secondary antibodies were used. Values are scaled for comparison to values in **e**. **g**, **h**, The same assay as in **f** except that responses to rh-CD4-Ig, lacking CCR5mim2 (**g**) or to CCR5mim2 fused to a human IgG1 Fc domain (**h**) were measured. Experiments in **c**–**h** were performed at least twice with similar results. Errors bars denote one s.e.m. of duplicates.

indicating that the eCD4-Ig was efficiently sulfated and fully active *in vivo*. We also compared macaque humoral responses to expressed rh-eCD4-Ig and to four AAV-expressed bNAbs inoculated for a separate study. 3BNC117, NIH45-45, 10-1074 and PGT121, each bearing rhesus IgG2 and light-chain constant domains, elicited markedly higher endogenous antibody responses than did rh-eCD4-Ig, consistent with their high levels of somatic hypermutation (Fig. 4e). To investigate the target of the anti-rh-eCD4-Ig responses, we increased the sensitivity of our assay and compared longitudinally the reactivity of inoculated rhesus sera to a series of antigens. rh-eCD4-Ig (Fig. 4f) and rh-CD4-Ig (without the CCR5mim2 sulfopeptide; Fig. 4g) were recognized by rhesus sera with nearly the same reactivity, whereas CCR5mim2 fused to a human IgG1 Fc domain was not (Fig. 4h), indicating that the sulfopeptide was not immunogenic. Rhesus CD4 domains 1 and 2 fused to a human IgG1 Fc was much less reactive than the same CD4 domains fused to the rhesus IgG2 Fc, without or with the Ile39Asn mutation (Extended Data Fig. 8e, f), whereas an unrelated construct bearing the rhesus IgG2 Fc domain showed no reactivity (Extended Data Fig. 8g), suggesting that a neo-epitope formed by the rhesus CD4 and Fc domains was recognized by most anti-rh-eCD4-Ig antibodies. Thus eCD4-Ig is less immunogenic than bNAbs, and can be expressed for at least 40 weeks at concentrations that are well tolerated and protective against several robust SHIV-AD8 challenges.

A key question is whether eCD4-Ig or a similar construct could be used to prevent new HIV-1 infections in a population, and whether it might do so more effectively than a bNAb. We show that AAV-delivered rhesus eCD4-Ig protected all inoculated macaques from multiple infectious doses that are probably higher than those present in most human transmission events, although we have not yet tested protection from mucosal challenges. Protection lasted at least 34 weeks after inoculation (Fig. 4b), and other studies indicate that these protective titres can be sustained for several years[2]. Previous studies of CD4-Ig indicate that it is safe when passively administered[12,14], and in particular it does not engage MHC II or otherwise interfere with immune function[13], although further safety studies of eCD4-Ig are warranted. eCD4-Ig has fewer non-self B- and T-cell epitopes than heavily hypermutated bNAbs, and thus elicits fewer endogenous antibodies that can impair its expression and activity (Fig. 4e). Its most prominent non-self element is its sulfopeptide, which did not elicit any measurable antibody responses (Fig. 4f–h). However, the clearest advantage of eCD4-Ig over bNAbs is its potency and its unmatched breadth (Fig. 3 and Extended Data Figs 4–7). The breadth of eCD4-Ig arises from the necessary conservation of its binding sites on Env, suggesting that emergence of eCD4-Ig escape variants in a population is less likely than with bNAbs. Moreover, any virus that does bypass prophylaxis is likely to bind CD4 and CCR5 less efficiently in the continued presence of eCD4-Ig, and may therefore be less efficiently retransmitted. Its potency suggests that relatively lower concentrations of eCD4-Ig will be sufficient to protect against most circulating viruses, a feature that may be critical to its use with AAV in humans. Although there are remaining challenges, these observations suggest that AAV-expressed eCD4-Ig could provide effective, long-term and near universal protection from HIV-1.

Online Content Methods, along with any additional Extended Data display items and Source Data, are available in the online version of the paper; references unique to these sections appear only in the online paper.

Received 29 June 2013; accepted 27 January 2015.
Published online 18 February 2015.

1. Balazs, A. B. *et al.* Antibody-based protection against HIV infection by vectored immunoprophylaxis. *Nature* **481,** 81–84 (2011).
2. Johnson, P. R. *et al.* Vector-mediated gene transfer engenders long-lived neutralizing activity and protection against SIV infection in monkeys. *Nature Med.* **15,** 901–906 (2009).
3. Diskin, R. *et al.* Increasing the potency and breadth of an HIV antibody by using structure-based rational design. *Science* **334,** 1289–1293 (2011).
4. Huang, J. *et al.* Broad and potent neutralization of HIV-1 by a gp41-specific human antibody. *Nature* **491,** 406–412 (2012).
5. Walker, L. M. *et al.* Broad neutralization coverage of HIV by multiple highly potent antibodies. *Nature* **477,** 466–470 (2011).
6. Scheid, J. F. *et al.* Sequence and structural convergence of broad and potent HIV antibodies that mimic CD4 binding. *Science* **333,** 1633–1637 (2011).
7. Lewis, A. D., Chen, R., Montefiori, D. C., Johnson, P. R. & Clark, K. R. Generation of neutralizing activity against human immunodeficiency virus type 1 in serum by antibody gene transfer. *J. Virol.* **76,** 8769–8775 (2002).
8. Greig, J. A. *et al.* Intramuscular injection of AAV8 in mice and macaques is associated with substantial hepatic targeting and transgene expression. *PLoS ONE* **9,** e112268 (2014).

9. Rizzuto, C. D. *et al.* A conserved HIV gp120 glycoprotein structure involved in chemokine receptor binding. *Science* **280,** 1949–1953 (1998).
10. Huang, C. C. *et al.* Structures of the CCR5 N terminus and of a tyrosine-sulfated antibody with HIV-1 gp120 and CD4. *Science* **317,** 1930–1934 (2007).
11. Lagenaur, L. A., Villarroel, V. A., Bundoc, V., Dey, B. & Berger, E. A. sCD4–17b bifunctional protein: extremely broad and potent neutralization of HIV-1 Env pseudotyped viruses from genetically diverse primary isolates. *Retrovirology* **7,** 11 (2010).
12. Fletcher, C. V. *et al.* Nonlinear pharmacokinetics of high-dose recombinant fusion protein CD4-IgG2 (PRO 542) observed in HIV-1-infected children. *J. Allergy Clin. Immunol.* **119,** 747–750 (2007).
13. Hussey, R. E. *et al.* A soluble CD4 protein selectively inhibits HIV replication and syncytium formation. *Nature* **331,** 78–81 (1988).
14. Jacobson, J. M. *et al.* Single-dose safety, pharmacology, and antiviral activity of the human immunodeficiency virus (HIV) type 1 entry inhibitor PRO 542 in HIV-infected adults. *J. Infect. Dis.* **182,** 326–329 (2000).
15. Haim, H. *et al.* Soluble CD4 and CD4-mimetic compounds inhibit HIV-1 infection by induction of a short-lived activated state. *PLoS Pathog.* **5,** e1000360 (2009).
16. Moebius, U., Clayton, L. K., Abraham, S., Harrison, S. C. & Reinherz, E. L. The human immunodeficiency virus gp120 binding site on CD4: delineation by quantitative equilibrium and kinetic binding studies of mutants in conjunction with a high-resolution CD4 atomic structure. *J. Exp. Med.* **176,** 507–517 (1992).
17. Sullivan, N. *et al.* Determinants of human immunodeficiency virus type 1 envelope glycoprotein activation by soluble CD4 and monoclonal antibodies. *J. Virol.* **72,** 6332–6338 (1998).
18. Farzan, M. *et al.* Tyrosine sulfation of the amino terminus of CCR5 facilitates HIV-1 entry. *Cell* **96,** 667–676 (1999).
19. Farzan, M. *et al.* A tyrosine-sulfated peptide based on the N terminus of CCR5 interacts with a CD4-enhanced epitope of the HIV-1 gp120 envelope glycoprotein and inhibits HIV-1 entry. *J. Biol. Chem.* **275,** 33516–33521 (2000).
20. Dorfman, T., Moore, M. J., Guth, A. C., Choe, H. & Farzan, M. A tyrosine-sulfated peptide derived from the heavy-chain CDR3 region of an HIV-1-neutralizing antibody binds gp120 and inhibits HIV-1 infection. *J. Biol. Chem.* **281,** 28529–28535 (2006).
21. Choe, H. *et al.* Tyrosine sulfation of human antibodies contributes to recognition of the CCR5 binding region of HIV-1 gp120. *Cell* **114,** 161–170 (2003).
22. Chiang, J. J. *et al.* Enhanced recognition and neutralization of HIV-1 by antibody-derived CCR5-mimetic peptide variants. *J. Virol.* **86,** 12417–12421 (2012).
23. Ridgway, J. B., Presta, L. G. & Carter, P. 'Knobs-into-holes' engineering of antibody CH3 domains for heavy chain heterodimerization. *Protein Eng.* **9,** 617–621 (1996).
24. Kwong, J. A. *et al.* A tyrosine-sulfated CCR5-mimetic peptide promotes conformational transitions in the HIV-1 envelope glycoprotein. *J. Virol.* **85,** 7563–7571 (2011).
25. Seaman, M. S. *et al.* Tiered categorization of a diverse panel of HIV-1 Env pseudoviruses for assessment of neutralizing antibodies. *J. Virol.* **84,** 1439–1452 (2010).
26. Alpert, M. D. *et al.* A novel assay for antibody-dependent cell-mediated cytotoxicity against HIV-1- or SIV-infected cells reveals incomplete overlap with antibodies measured by neutralization and binding assays. *J. Virol.* **86,** 12039–12052 (2012).
27. Humes, D., Emery, S., Laws, E. & Overbaugh, J. A species-specific amino acid difference in the macaque CD4 receptor restricts replication by global circulating HIV-1 variants representing viruses from recent infection. *J. Virol.* **86,** 12472–12483 (2012).

Acknowledgements This project was supported by National Institutes of Health (NIH) grants R01 AI091476 and R01 AI080324 (M.F.), P01 AI100263 (G.G., R.C.D., M.F.), RR000168 (M.R.G., L.M.K., D.T.E., R.C.D., M.F.), R01 AI058715 (B.H.H.), by the Intramural Research program of the Vaccine Research Center, NIAID, NIH (J.G., B.Z., P.D.K.), and by federal funds from the National Cancer Institute, NIH under contract no. HHSN261200800001E. The authors would like to thank H. Choe and M. Martin for critical advice.

Author Contributions M.R.G. and L.M.K. contributed equally to this work. M.R.G., L.M.K., H.R.K., M.V.S., T.D., J.J.C., M.D.A., M.P., J.D.L., R.C.D., D.T.E., B.H.H., P.M.C., M.S.S., A.P. and M.F. designed experiments. M.R.G., L.M.K., H.R.K., M.V.S., T.D., J.J.C., K.G.H., J.M.D., M.D.A., C.C.B., C.H.F., V.R.J., B.D.Q. and A.Y.Y. performed experiments. L.M.K. conducted all non-human primate studies. J.G. and P.D.K. assisted with modelling. J.M.M.-N., H.M., B.Z., P.P., M.S.S., M.C.N. and D.R.B. contributed advice and critical reagents. M.F. conceived the study and, with important assistance from M.R.G. and L.M.K., wrote the manuscript.

Author Information Reprints and permissions information is available at www.nature.com/reprints. The authors declare no competing financial interests. Readers are welcome to comment on the online version of the paper. Correspondence and requests for materials should be addressed to M.F. (mfarzan@scripps.edu).

METHODS

Plasmids and cells. Plasmid expressing CD4-Ig was previously described[20]. Fusion constructs were created by adding sequences encoding CCR5mim1 and tetra-glycine linker to N terminus (fusion1) or between domain 2 and human Fc (fusion2) of CD4-Ig by inverse PCR. eCD4-Ig (fusion3) and eCD4-Ig^{mim2} were created by adding sequence encoding a tetra-glycine linker and CCR5mim1 or CCR5mim2, respectively, to the C terminus of CD4-Ig by inverse PCR. The Gln 40 to Ala mutation was introduced in eCD4-Ig and eCD4-Ig^{mim2} by Quickchange PCR. The eCD4-Ig/CD4-Ig heterodimer was generated as previously described[23] and analysed by SDS–PAGE under reducing and non-reducing conditions. rh-eCD4-Ig, consisting of rhesus CD4 domains 1 and 2 bearing an Ile39Asn mutation, rhesus IgG2 Fc and CCR5mim2, was synthesized and cloned into a previously described single-stranded AAV plasmid[2]. AAV expression plasmids for HIV-1 antibodies were created by synthesizing the variable heavy and light chains of 3BNC117, NIH45-46, PGT121 and 10-1074 with the rhesus heavy and light constant regions, and cloning these genes into a previously described ssAAV plasmid[2]. The following reagent was obtained through the NIH AIDS Reagent Program (Division of AIDS, NIAID, NIH): CMVR-VRC01-H, CMVR-VRC01-L, from J. Mascola[28,29], pNL4-3.Luc.R-.E- from N. Landeau[30,31], TZM-bl cells from J. C. Kappes, X. Wu and Tranzyme Inc[32–36], SF162 gp160 from L. Stamatatos and C. Cheng-Mayer[37], and GHOST-CCR5 and -CXCR4-cells from V. KewalRamani and D. Littman. Human embryonic kidney HEK293T cells were obtained from ATCC. Cf2Th-CD4$^+$.CCR5$^+$ and CfTh-CCR5$^+$ cells were a gift from H. Choe. No testing for mycoplasma contamination was performed in any cell line after their receipt from these contributors. The variable heavy and light chains of IgG-b12, NIH45-46, 3BNC117, 10-1074 and PGT121 were cloned into the CMVR-VRC01-H and -L plasmids. Plasmids encoding TPST-2 or the envelope glycoproteins pNL4-3Δenv, 89.6, ADA, SG3, SA32, YU2, JRFL, KB9, VSV-G, HIV-2 ST, SIVmac239, SIVmac316 and replicative 89.6 or SG3 viruses were previously described[20,21,38–40].

Purification of antibodies, CD4–Ig and eCD4-Ig variants. Production of CD4-Ig, eCD4-Ig variants and antibodies was performed as previously described[41]. In brief, HEK293T cells in 140 mm plates were transfected with 25 μg per plate at 50% confluency by the calcium phosphate transfection method. Plasmids encoding sulfated proteins were cotransfected with a plasmid encoding human tyrosine protein sulfotranserase 2 (TPST2). At 12 h after transfection, 10% FBS-DMEM media was replaced with serum-free 293 Freestyle media (Invitrogen). Media was collected after 48 h, debris was cleared by centrifugation for 10 min at 1,500*g* and filtered using 0.45-μm filter flasks (Millipore). Complete protease inhibitor cocktail (Roche) was added to the filtered supernatants. A 500-μl bed volume of Protein A sepharose beads (GE Healthcare) was added and agitated at 4 °C overnight. The bead–media mixture was collected by gravity flow column (Biorad) and was washed with 30 ml PBS (Lonza) plus 0.5 M NaCl (0.65 M NaCl final) followed by 10 ml PBS. Protein was eluted with 3 M $MgCl_2$ in PBS. Buffer was exchanged for PBS and protein was concentrated to 1 mg ml^{-1} by Ultrafiltration (Amicon Ultra) at 4,000*g*.

Flow cytometry analysis of CD4-Ig and eCD4-Ig binding to cell-expressed envelope glycoprotein. HEK293T cells were transfected with plasmids expressing envelope glycoprotein lacking cytoplasmic residues 732 to 876 (HXBc2 numbering) together with plasmid encoding the tat protein. Transfection medium was replaced after an overnight incubation and cells were collected 48 h after transfection. Collected cells were washed twice in flow cytometry buffer (PBS with 2% goat serum, 0.01% sodium azide). Cells were incubated with CD4-Ig or eCD4-Ig on ice for 1 h and then washed twice with flow cytometry buffer. A secondary antibody recognizing human Fc (Jackson Immuno Research) was added to the cells for 30 min. Cells were washed twice with flow cytometry buffer, twice with PBS, and resuspended in 1% paraformaldehyde solution. Binding was analysed with an Accuri C6 Flow Cytometer (BD Biosciences) and data analysed with the C6 Software (BD Biosciences).

Viral entry enhancement assay. HIV-1 pseudovirus expressing firefly luciferase was pre-incubated with titrated amounts of CD4-Ig or eCD4-Ig variants in DMEM (10% FBS) for 1 h at 37 °C. CD4-negative Cf2Th-CCR5 cells were collected and diluted in DMEM (10% FBS) to 100,000 cells ml^{-1} and added to the pseudovirus/inhibitor mixture. Cells were then incubated for 48 h at 37 °C. Viral entry was analysed using Britelite Plus (Perkin Elmer) and luciferase activity of cell lysates was read using a Victor X3 plate reader (Perkin Elmer).

HIV-1 neutralization assays. GHOST-CCR5 or -CXCR4 cells were plated into 12-well plates at 50,000 cells per well. HIV-1 pseudovirus was diluted in RPMI and titrated amounts of CD4-Ig, fusion1, fusion2 or eCD4-Ig were added. Virus and inhibitor were incubated at room temperature for 20 min and added to the cells for 2 h at 37 °C. Cells were then washed with serum-free medium and then incubated in 1 ml of DMEM (10% FBS) for 48 h at 37 °C. Cells were collected by trypsinization, fixed in 1% paraformaldehyde in PBS, and viral entry was determined by flow cytometry based on GFP expression.

For studies of infectious virus, unstimulated PBMCs were collected and resuspended in RPMI medium (15% FBS, 20 U ml^{-1} IL-2). Cells were plated in a 12-well plate at 10^6 cells per well. HIV-1 was diluted in RPMI and varying amounts of inhibitor were added. The virus and inhibitor was incubated at room temperature for 20 min and added to the cells for 3 h at 37 °C. Cells were then washed with serum-free medium and resuspended in fresh RPMI medium (15% FBS, 20 U ml^{-1} IL-2). At 3-day intervals after infection, supernatants were collected and fresh RPMI medium (15% FBS, 20 U ml^{-1} IL-2) was added to the cells. Supernatants were analysed for viral infection by ELISA with Alliance HIV-1 p24 antigen ELISA kit (Perkin Elmer).

TZM-bl neutralization assays were performed as previously described[42]. In brief, HIV-1 pseudoviruses were pre-incubated with titrated amounts of CD4-Ig or eCD4-Ig variants in DMEM (10% FBS) for 1 h at 37 °C. TZM-bl cells were collected and diluted in DMEM (10% FBS) to 100,000 cells ml^{-1} and added to the pseudovirus/inhibitor mixture. Cells were then incubated for 48 h at 37 °C. Viral entry was analysed using Britelite Plus (Perkin Elmer) and luciferase activity was read using a Victor X3 plate reader (Perkin Elmer). All neutralization and enhancement studies of Figs 1–4 were performed at least twice in triplicate. All error bars represent s.e.m.

Antibody-dependent cell-mediated cytotoxicity assays. ADCC activity was performed as previously described[43]. In brief, CEM.NKR CCR5 CD4$^+$ T cells were infected 4 days with infectious HIV-1 NL4.3, SHIV-KB9 or SIVmac239. After 4 days, KHYG-1 effector cells were co-incubated with infected cells in the presence of titrated CD4-Ig, eCD4-Ig variants, or the b12 antibody for 8 h. ADCC activity was measured by luciferase activity as above.

Production of HIV-1_{NL4-3} stocks and SHIV-AD8-EO stocks for *in vivo* studies. A molecular clone of HIV-1_{NL4-3} was obtained from the AIDS Research and Reference Reagent Program (ARRRP), Division of AIDS, NIAID, NIH from material deposited by S. Gartner, M. Popovic, R. Gallo and M. Martin. Virus stocks were produced in 293T cells by transient transfection using TurboFect (Thermo Scientific) and 12 μg of proviral plasmid. Supernatants were collected at 40 h, filtered through 0.45-μm filters, and dispensed into single use doses and frozen at −80 °C. Viruses were quantified by p24 ELISA (Zeptometrix) and by GHOST cell titer[44] to determine infectious units per millilitre (IU ml^{-1}). Titering was performed per the GHOST cell line protocol obtained through ARRRP. The molecular clone of SHIV-AD8-EO was a gift from M. Martin[45]. 293T cells were plated in 140 mm flasks and transfected with 80 μg DNA per plate by calcium phosphate technique. At 12 h after transfection, flasks were replaced with fresh DMEM (10% FBS). Medium was collected at 48 h after transfection, frozen at −80 °C, and titred using an SIV p27 ELISA kit (ABL).

Haematopoietic stem cell isolation and NSG mouse transplantation. Human CD34$^+$ haematopoietic stem cells were isolated from fetal livers obtained from Advanced Bioscience Resources, INC (ABR). Tissue was disrupted and incubated with 1 mg ml^{-1} collagenase/dispase (Roche Applied Sciences) for 15 min at 37 °C. Cells were isolated by passing the disrupted tissue through a 70-μm filter. Red blood cells were lysed in BD Pharm Lyse (BD Biosciences), with CD34$^+$ cells being isolated using CD34 MACS microbeads (Miltenyi) according to manufacturer's instructions with an additional purification step using a second column. NOD.Cg-Prkdc scid Il2rγ tm1Wj/Szj (NOD/SCID/*Il2rg*$^{-/-}$, NSG) mice were obtained from Jackson Laboratories. Neonatal mice received 150 cGy radiation, and 2–4 h later 1×10^6 CD34$^+$ haematopoietic stem cells in 1% heparin (Celgene) via intrahepatic injection. Mice were monitored for engraftment levels of human CD45$^+$ cells and development of T cells and B cells at 8, 10 and 12 weeks after engraftment.

Mouse infections, treatment and analysis. Humanized mice with evidence of human CD4$^+$ T-cell development in blood were infected with 5×10^4 IU of HIV-1NL4.3 by intraperitoneal injection. Mice were administered with 65 μg of eCD4-Ig once weekly for the first 2 weeks, starting at 8 days before the HIV-1 challenge, and then twice weekly starting at week 3 by retro-orbital injection while under anaesthetization by 2.5% isoflurane. Mock-treated mice received a retro-orbital injection of PBS 1 and 8 days before HIV-1 challenge, and were anaesthetized in parallel with eCD4-Ig mice throughout. Every week after infection the mice were anaesthetized by inhalation of 2.5% isoflurane and blood was collected retro-orbitally for analysis. At week 6, three eCD4-Ig-treated mice and one mock-treated mouse (who had not become infected) were challenged a second time with 5×10^4 IU HIV-1 NL4-3. Mouse blood was blocked for 20 min at room temperature in FBS (Denville) and stained with appropriate antibodies for 15 min at room temperature. Red blood cells were removed by incubation in BD FACS Fix/Lysing Solution (BD Biosciences), which was removed by dilution with PBS before analysis by flow cytometry. HIV-1 levels in peripheral blood were determined by extracting viral RNA from mouse plasma at each blood draw using a viral RNA isolation kit (Qiagen) followed by Taqman One-Step RT–PCR (Life Technologies) using a primer and probe set targeting the HIV-1 LTR region, as previously described[46,47]. Reactions were performed and analysed using a 7500 Fast Realtime PCR System (Life Technologies). To analyse engrafted T cells by flow cytometry, stained cells were acquired on a FACS Canto II (BD Biosciences) and analysed using FlowJo software v7.6.5 (Tree

Star Inc.). Blood samples were stained using human-specific antibodies at a 1:20 dilution for CD4-V450 (RPA-T4), CD8-APC (RPAT8), CD3-PE (UCHT1) and CD45-PerCP (TUI16) (BD Bioscience). Up to 10,000 events were recorded for viable cell populations and gated based on fluorescence minus one controls as previously described[46]. All mouse studies were performed in accordance with the Scripps Research Institute Institutional Review Board, protocol number 14-018. No statistical methods were used to predetermine sample size.

AAV inoculation of rhesus macaques. Eight 4-year-old AAV1-negative male Indian-origin rhesus macaques were housed at the New England Primate Research Center in accordance with standards set forth by the American Association for Accreditation of Laboratory Animal Care. Their weights at the time of AAV inoculation ranged from 5.2 to 8.2 kg. Macaques were separated into age- and weight-matched control groups, but blinding and randomization were not performed. Four macaques were inoculated with 1 ml RPMI containing 2.5×10^{13} AAV1 particles delivering 80% of a single-strand rh-eCD4-Ig transgene (IgG2 isotype) and 20% of a single-strand rhesus TPST-2 transgene into each quadriceps muscle (two 0.5 ml per injections per quadriceps muscle). Five millilitres of sera was obtained every 1–2 weeks after AAV inoculation beginning at week 4. Animals were challenged at week 8 after inoculation with 2 pg p27 of SHIV-AD8-EO. SHIV-negative animals were repeatedly challenged with escalating doses of SHIV-AD8-EO up to 800 pg p27. Plasma viral loads were quantified as previously described[45].

For AAV studies of bNAbs, six 2-year-old AAV1-negative Indian-origin rhesus macaques (two males and four females) were housed at the New England Primate Research Center in accordance with standards set forth by the American Association for Accreditation of Laboratory Animal Care. Three macaques were inoculated with 1 ml RPMI containing 1×10^{13} AAV1 particles delivering single-strand rh-3BNC117-IgG2 transgene into one quadriceps (two 0.5-ml injections) and 1 ml RPMI containing 1×10^{13} AAV1 particles delivering single-stranded rh-10-1074-IgG2 transgene into the contralateral quadriceps (two 0.5-ml injections). The other three macaques were inoculated with 1 ml RPMI containing 1×10^{13} AAV1 particles delivering single-strand rh-NIH45-46-IgG2 transgene into one quadriceps (two 0.5-ml injections) and 1 ml RPMI containing 1×10^{13} AAV1 particles delivering single-strand rh-PGT121-IgG2 transgene into the contralateral quadriceps (two 0.5-ml injections). Five millilitres of sera was obtained every 2 weeks beginning at week 2 and analysed by ELISA. All primate studies were performed in accordance with the Harvard Medical School Standing Committee on Animals protocol number 04888.

eCD4-Ig, rh-eCD4-Ig and anti-transgene antibody concentrations in NSG mice and rhesus macaque sera. *In vivo* concentrations of eCD4-Ig, rh-eCD4-Ig were measured by ELISA as previously described[2]. In brief, to measure NSG mouse and macaque serum concentrations, ELISA plates (Costar) were coated with 5 μg ml^{-1} SIV gp120 overnight at 4 °C. Plates were washed with PBS-T (PBS plus 0.05% Tween-20) twice and blocked with 5% milk in PBS for 1 h at 37 °C. Sera serially diluted in 5% milk in PBS were added to the plate and incubated for 1 h at 37 °C. Samples were washed five times with PBS-T and a horseradish peroxidase secondary antibody (Jackson Immuno Research) recognizing human IgG1. Plates were incubated for 1 h at 37 °C and then washed ten times with PBS-T. TMB solution (Fisher) was added for 10 min at room temperature and then stopped with TMB Stop Solution (Southern Biotech). Absorbance was read at 450 nm by a Victor X3 plate reader (Perkin Elmer) and compared with a standard curve generated using a rh-eCD4-Ig mixed with pre-inoculation sera. Anti-rh-eCD4-Ig antibodies and anti-bNAb antibodies were measured in the same way except that ELISA plates were coated with 5 μg ml^{-1} of various constructs. Constructs so assayed included rh-eCD4-Ig, rh-CD4-Ig^{I39N}, rh-CD4-Ig domains 1 and 2 (with or without Ile39Asn) bearing a human IgG1 Fc and hinge domain, C-terminal CCR5mim2-Ig (human IgG1 Fc and hinge, no CD4 domains), NIH45-46 bearing the rhesus IgG2 Fc domain and hinge, or HIV-1 bNAbs. Serum samples were diluted 10- or 20-fold and blocked in 5% milk in PBS. Anti-transgene antibodies were measured using secondary antibodies detecting either the kappa or lambda light chain (Southern Biotech) that was opposite of the antibody being assayed when comparing the anti-bNAb response to that to rh-eCD4-Ig. Both anti-kappa and anti-lambda secondary antibodies were used when measuring anti-rh-eCD4-Ig responses alone. TMB solution was added for 10–15 min at room temperature and measured as described above.

28. Wu, X. *et al.* Rational design of envelope identifies broadly neutralizing human monoclonal antibodies to HIV-1. *Science* **329,** 856–861 (2010).
29. Barouch, D. H. *et al.* A human T-cell leukemia virus type 1 regulatory element enhances the immunogenicity of human immunodeficiency virus type 1 DNA vaccines in mice and nonhuman primates. *J. Virol.* **79,** 8828–8834 (2005).
30. He, J. *et al.* Human immunodeficiency virus type 1 viral protein R (Vpr) arrests cells in the G2 phase of the cell cycle by inhibiting p34cdc2 activity. *J. Virol.* **69,** 6705–6711 (1995).
31. Connor, R. I., Chen, B. K., Choe, S. & Landau, N. R. Vpr is required for efficient replication of human immunodeficiency virus type-1 in mononuclear phagocytes. *Virology* **206,** 935–944 (1995).
32. Platt, E. J., Bilska, M., Kozak, S. L., Kabat, D. & Montefiori, D. C. Evidence that ecotropic murine leukemia virus contamination in TZM-bl cells does not affect the outcome of neutralizing antibody assays with human immunodeficiency virus type 1. *J. Virol.* **83,** 8289–8292 (2009).
33. Takeuchi, Y., McClure, M. O. & Pizzato, M. Identification of gammaretroviruses constitutively released from cell lines used for human immunodeficiency virus research. *J. Virol.* **82,** 12585–12588 (2008).
34. Wei, X. *et al.* Emergence of resistant human immunodeficiency virus type 1 in patients receiving fusion inhibitor (T-20) monotherapy. *Antimicrob. Agents Chemother.* **46,** 1896–1905 (2002).
35. Derdeyn, C. A. *et al.* Sensitivity of human immunodeficiency virus type 1 to the fusion inhibitor T-20 is modulated by coreceptor specificity defined by the V3 loop of gp120. *J. Virol.* **74,** 8358–8367 (2000).
36. Platt, E. J., Wehrly, K., Kuhmann, S. E., Chesebro, B. & Kabat, D. Effects of CCR5 and CD4 cell surface concentrations on infections by macrophagetropic isolates of human immunodeficiency virus type 1. *J. Virol.* **72,** 2855–2864 (1998).
37. Harouse, J. M. *et al.* Mucosal transmission and induction of simian AIDS by CCR5-specific simian/human immunodeficiency virus SHIV(SF162P3). *J. Virol.* **75,** 1990–1995 (2001).
38. Choe, H. *et al.* The orphan seven-transmembrane receptor apj supports the entry of primary T-cell-line-tropic and dualtropic human immunodeficiency virus type 1. *J. Virol.* **72,** 6113–6118 (1998).
39. Choe, H. *et al.* The beta-chemokine receptors CCR3 and CCR5 facilitate infection by primary HIV-1 isolates. *Cell* **85,** 1135–1148 (1996).
40. Farzan, M. *et al.* A tyrosine-rich region in the N terminus of CCR5 is important for human immunodeficiency virus type 1 entry and mediates an association between gp120 and CCR5. *J. Virol.* **72,** 1160–1164 (1998).
41. Quinlan, B. D., Gardner, M. R., Joshi, V. R., Chiang, J. J. & Farzan, M. Direct expression and validation of phage-selected peptide variants in mammalian cells. *J. Biol. Chem.* **288,** 18803–18810 (2013).
42. Li, M. *et al.* Human immunodeficiency virus type 1 Env clones from acute and early subtype B infections for standardized assessments of vaccine-elicited neutralizing antibodies. *J. Virol.* **79,** 10108–10125 (2005).
43. Alpert, M. D. *et al.* ADCC develops over time during persistent infection with live-attenuated SIV and is associated with complete protection against $SIV_{mac}251$ challenge. *PLoS Pathog.* **8,** e1002890 (2012).
44. Mörner, A. *et al.* Primary human immunodeficiency virus type 2 (HIV-2) isolates, like HIV-1 isolates, frequently use CCR5 but show promiscuity in coreceptor usage. *J. Virol.* **73,** 2343–2349 (1999).
45. Shingai, M. *et al.* Antibody-mediated immunotherapy of macaques chronically infected with SHIV suppresses viraemia. *Nature* **503,** 277–280 (2013).
46. Holt, N. *et al.* Human hematopoietic stem/progenitor cells modified by zinc-finger nucleases targeted to CCR5 control HIV-1 in vivo. *Nature Biotechnol.* **28,** 839–847 (2010).
47. Rouet, F. *et al.* Transfer and evaluation of an automated, low-cost real-time reverse transcription-PCR test for diagnosis and monitoring of human immunodeficiency virus type 1 infection in a West African resource-limited setting. *J. Clin. Microbiol.* **43,** 2709–2717 (2005).
48. Tran, E. E. *et al.* Structural mechanism of trimeric HIV-1 envelope glycoprotein activation. *PLoS Pathog.* **8,** e1002797 (2012).
49. Sauer-Eriksson, A. E., Kleywegt, G. J., Uhlen, M. & Jones, T. A. Crystal structure of the C2 fragment of streptococcal protein G in complex with the Fc domain of human IgG. *Structure* **3,** 265–278 (1995).
50. Huang, C. C. *et al.* Structural basis of tyrosine sulfation and VH-gene usage in antibodies that recognize the HIV type 1 coreceptor-binding site on gp120. *Proc. Natl Acad. Sci. USA* **101,** 2706–2711 (2004).

Key: Leader sequences (underlined), CD4 domains 1 and 2 (red), linker regions (black), antibody hinge and Fc regions (cyan), CCR5-mimetic sequences (green), and mutations (grey highlight).

CD4-Ig CD5 leader sequence (human); CD4 domains 1 and 2 (human); short AADP linker; IgG1 hinge and Fc (human).

MPMGSLQPLATLYLLGMLVASVLAKKVVLGKKGDTVELTCTASQKKSIQFHWKNSNQIKILGNQGSFLTKGPSKLNDRADSRRSLWDQGNFPLIIKNLKIEDSDTYIC
EVEDQKEEVQLLVFGLTANSDTHLLQGQSLTLTLESPPGSSPSVQCRSPRGKNIQGGKTLSVSQLELQDSGTWTCTVLQNQKKVEFKIDIVVLAAADPEPKSCDKTHT
CPPCPAPELLGGPSVFLFPPKPKDTLMISRTPEVTCVVVDVSHEDPEVKFNWYVDGVEVHNAKTKPREEQYNSTYRVVSVLTVLHQDWLNGKEYKCKVSNKALPAPIE
KTISKAKGQPREPQVYTLPPSRDELTKNQVSLTCLVKGFYPSDIAVEWESNGQPENNYKTTPPVLDSDGSFFLYSKLTVDKSRWQQGNVFSCSVMHEALHNHYTQKSL
SLSPGK

eCD4-Ig CD5 leader sequence (human); CD4 domains 1 and 2 (human); short AADP linker; IgG1 hinge and Fc (human); tetraglycine linker; CCR5mim1.

MPMGSLQPLATLYLLGMLVASVLAKKVVLGKKGDTVELTCTASQKKSIQFHWKNSNQIKILGNQGSFLTKGPSKLNDRADSRRSLWDQGNFPLIIKNLKIEDSDTYIC
EVEDQKEEVQLLVFGLTANSDTHLLQGQSLTLTLESPPGSSPSVQCRSPRGKNIQGGKTLSVSQLELQDSGTWTCTVLQNQKKVEFKIDIVVLAAADPEPKSCDKTHT
CPPCPAPELLGGPSVFLFPPKPKDTLMISRTPEVTCVVVDVSHEDPEVKFNWYVDGVEVHNAKTKPREEQYNSTYRVVSVLTVLHQDWLNGKEYKCKVSNKALPAPIE
KTISKAKGQPREPQVYTLPPSRDELTKNQVSLTCLVKGFYPSDIAVEWESNGQPENNYKTTPPVLDSDGSFFLYSKLTVDKSRWQQGNVFSCSVMHEALHNHYTQKSL
SLSPGKGGGGGDYADYDGGYYYDMD

Fusion 1 CD5 leader sequence (human); CCR5mim1; tetraglycine linker; CD4 domains 1 and 2 (human); short AADP linker; IgG1 hinge and Fc (human).

MPMGSLQPLATLYLLGMLVASVLAGDYADYDGGYYYDMDGGGGKKVVLGKKGDTVELTCTASQKKSIQFHWKNSNQIKILGNQGSFLTKGPSKLNDRADSRRSLWDQG
NFPLIIKNLKIEDSDTYICEVEDQKEEVQLLVFGLTANSDTHLLQGQSLTLTLESPPGSSPSVQCRSPRGKNIQGGKTLSVSQLELQDSGTWTCTVLQNQKKVEFKID
IVVLAAADPEPKSCDKTHTCPPCPAPELLGGPSVFLFPPKPKDTLMISRTPEVTCVVVDVSHEDPEVKFNWYVDGVEVHNAKTKPREEQYNSTYRVVSVLTVLHQDWL
NGKEYKCKVSNKALPAPIEKTISKAKGQPREPQVYTLPPSRDELTKNQVSLTCLVKGFYPSDIAVEWESNGQPENNYKTTPPVLDSDGSFFLYSKLTVDKSRWQQGNV
FSCSVMHEALHNHYTQKSLSLSPGK

Fusion 2 CD5 leader sequence (human); CD4 domains 1 and 2 (human); short AA linker; tetraglycine linker; CCR5mim1; short DP linker; IgG1 hinge and Fc (human)

MPMGSLQPLATLYLLGMLVASVLAKKVVLGKKGDTVELTCTASQKKSIQFHWKNSNQIKILGNQGSFLTKGPSKLNDRADSRRSLWDQGNFPLIIKNLKIEDSDTYIC
EVEDQKEEVQLLVFGLTANSDTHLLQGQSLTLTLESPPGSSPSVQCRSPRGKNIQGGKTLSVSQLELQDSGTWTCTVLQNQKKVEFKIDIVVLAAAGGGGGDYADYDG
GYYYDMDDPEPKSCDKTHTCPPCPAPELLGGPSVFLFPPKPKDTLMISRTPEVTCVVVDVSHEDPEVKFNWYVDGVEVHNAKTKPREEQYNSTYRVVSVLTVLHQDWL
NGKEYKCKVSNKALPAPIEKTISKAKGQPREPQVYTLPPSRDELTKNQVSLTCLVKGFYPSDIAVEWESNGQPENNYKTTPPVLDSDGSFFLYSKLTVDKSRWQQGNV
FSCSVMHEALHNHYTQKSLSLSPGK

eCD4-Ig^{mim2} CD5 leader sequence (human); CD4 domains 1 and 2 (human); short AADP linker; IgG1 hinge and Fc (human); tetraglycine linker; CCR5mim2 (Y4A difference from CCR5mim1 highlighted).

MPMGSLQPLATLYLLGMLVASVLAKKVVLGKKGDTVELTCTASQKKSIQFHWKNSNQIKILGNQGSFLTKGPSKLNDRADSRRSLWDQGNFPLIIKNLKIEDSDTYIC
EVEDQKEEVQLLVFGLTANSDTHLLQGQSLTLTLESPPGSSPSVQCRSPRGKNIQGGKTLSVSQLELQDSGTWTCTVLQNQKKVEFKIDIVVLAAADPEPKSCDKTHT
CPPCPAPELLGGPSVFLFPPKPKDTLMISRTPEVTCVVVDVSHEDPEVKFNWYVDGVEVHNAKTKPREEQYNSTYRVVSVLTVLHQDWLNGKEYKCKVSNKALPAPIE
KTISKAKGQPREPQVYTLPPSRDELTKNQVSLTCLVKGFYPSDIAVEWESNGQPENNYKTTPPVLDSDGSFFLYSKLTVDKSRWQQGNVFSCSVMHEALHNHYTQKSL
SLSPGKGGGGGDYYDYDGGYYYDMD

eCD4-Ig^{Q40A} CD5 leader sequence (human); CD4 domains 1 and 2 (human) with Q40A mutation (highlighted); short AADP linker; IgG1 hinge and Fc (human); tetraglycine linker; CCR5mim1.

MPMGSLQPLATLYLLGMLVASVLAKKVVLGKKGDTVELTCTASQKKSIQFHWKNSNQIKILGNAGSFLTKGPSKLNDRADSRRSLWDQGNFPLIIKNLKIEDSDTYIC
EVEDQKEEVQLLVFGLTANSDTHLLQGQSLTLTLESPPGSSPSVQCRSPRGKNIQGGKTLSVSQLELQDSGTWTCTVLQNQKKVEFKIDIVVLAAADPEPKSCDKTHT
CPPCPAPELLGGPSVFLFPPKPKDTLMISRTPEVTCVVVDVSHEDPEVKFNWYVDGVEVHNAKTKPREEQYNSTYRVVSVLTVLHQDWLNGKEYKCKVSNKALPAPIE
KTISKAKGQPREPQVYTLPPSRDELTKNQVSLTCLVKGFYPSDIAVEWESNGQPENNYKTTPPVLDSDGSFFLYSKLTVDKSRWQQGNVFSCSVMHEALHNHYTQKSL
SLSPGKGGGGGDYADYDGGYYYDMD

eCD4-Ig^{Q40A,mim2} CD5 leader sequence (human); CD4 domains 1 and 2 (human) with Q40A mutation (highlighted); short AADP linker; IgG1 hinge and Fc (human); tetraglycine linker; CCR5mim2 (difference from CCR5mim1 highlighted).

MPMGSLQPLATLYLLGMLVASVLAKKVVLGKKGDTVELTCTASQKKSIQFHWKNSNQIKILGNAGSFLTKGPSKLNDRADSRRSLWDQGNFPLIIKNLKIEDSDTYIC
EVEDQKEEVQLLVFGLTANSDTHLLQGQSLTLTLESPPGSSPSVQCRSPRGKNIQGGKTLSVSQLELQDSGTWTCTVLQNQKKVEFKIDIVVLAAADPEPKSCDKTHT
CPPCPAPELLGGPSVFLFPPKPKDTLMISRTPEVTCVVVDVSHEDPEVKFNWYVDGVEVHNAKTKPREEQYNSTYRVVSVLTVLHQDWLNGKEYKCKVSNKALPAPIE
KTISKAKGQPREPQVYTLPPSRDELTKNQVSLTCLVKGFYPSDIAVEWESNGQPENNYKTTPPVLDSDGSFFLYSKLTVDKSRWQQGNVFSCSVMHEALHNHYTQKSL
SLSPGKGGGGGDYYDYDGGYYYDMD

rh-eCD4-Ig (rh-eCD4-IgG2^{I39N,mim2}) CD4 leader sequence (rhesus); CD4 domains 1 and 2 (rhesus) with I39N mutation (highlighted); IgG2 hinge and Fc (rhesus); tetraglycine linker; CCR5mim2 (difference from CCR5mim1 highlighted).

MNRGIPFRHLLLVLQLALLPAVTQGKKVVLGKKGDTVELTCNASQKKNTQFHWKNSNQIKILGNQGSFLTKGPSKLSDRADSRKSLWDQGCFSMIIKNLKIEDSDTYI
CEVENKKEEVELLVFGLTANSDTHLLEGQSLTLTLESPPGSSPSVKCRSPGGKNIQGGRTISVPQLERQDSGTWTCTVSQDQKTVEFKIDIVVLAFQKASSTGLPCRS
TCPPCPAELLGGPSVFLFPPKPKDTLMISRTPEVTCVVVDVSQEEPDVKFNWYVDGVEVHNAQTKPREEQFNSTYRVVSVLTVTHQDWLNGKEYTCKVSNKALPAPRQ
KTVSKTKGQPREPQVYTLPPPREELTKNQVSLTCLVKGFYPSDIVVEWASNGQPENTYKTTPPVLDSDGSYFLYSKLTVDKSRWQQGNTFSCSVMHEALHNHYTQKSL
SVSPGKGGGGGDYYDYDGGYYYDMD

Extended Data Figure 1 | Sequences of CD4-Ig and eCD4-Ig variants. The amino-acid sequences of CD4-Ig, eCD4-Ig, fusion1, fusion2, eCD4-Ig^{mim2}, eCD4-Ig^{Q40A}, eCD4-Ig^{Q40A,mim2} and rh-eCD4-Ig (rh-eCD4-IgG2^{I39N,mim2}) are shown. Leader peptides are underlined, CD4 domains 1 and 2 are indicated in red, Fc domains are indicated in cyan, CCR5-mimetics peptides are indicated in green, and linker sequences are shown in black.

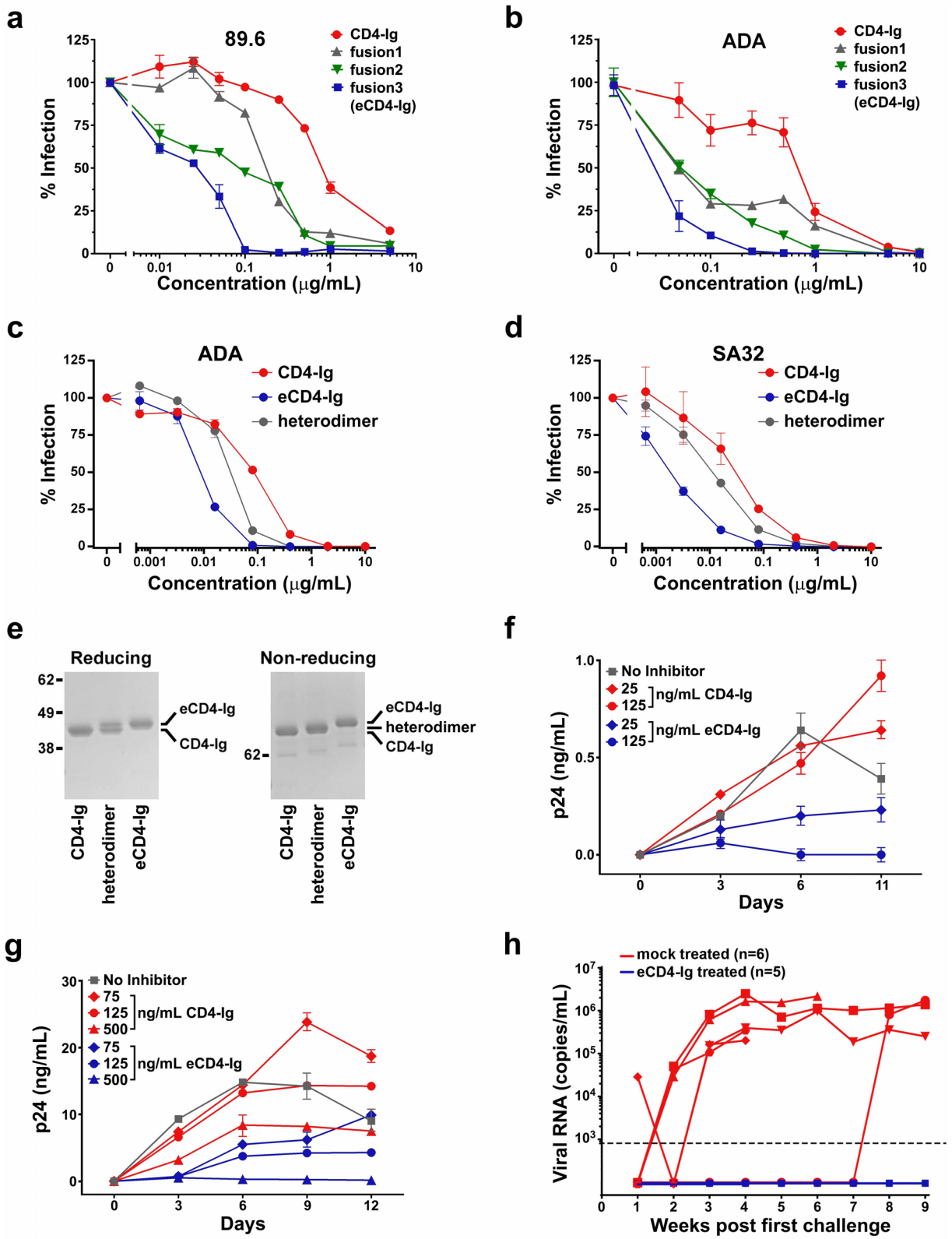

Extended Data Figure 2 | Additional characterization of eCD4-Ig. **a**, **b**, Experiments similar to those of Fig. 1b except that CD4-Ig (red), fusion1 (grey), fusion2 (green) and fusion3 (eCD4-Ig; blue) are compared using HIV-1 pseudotyped with the envelope glycoproteins of the 89.6 (**a**) or ADA (**b**) isolates. **c**, **d**, Experiments similar to those in Fig. 1e except that CD4-Ig (red), eCD4-Ig (blue) or heterodimers thereof (grey) are compared. **e**, CD4-Ig, eCD4-Ig and the CD4-Ig/eCD4-Ig heterodimer assayed in **c**, **d** and Fig. 1e were analysed by SDS–PAGE and stained with Coomassie blue under reducing (left) and non-reducing (right) conditions. **f**, **g**, Infectious 89.6 (**f**) or SG3 (**g**) HIV-1 was incubated with human PBMC in the presence of the indicated concentrations of CD4-Ig (red) or eCD4-Ig (blue), or without either inhibitor (grey). Culture supernatants were collected on the indicated day and viral p24 levels were measured by ELISA. **h**, Viral loads in RNA copies ml^{-1} are shown for each humanized mouse of Fig. 1f. Mice treated with eCD4-Ig are indicated with blue lines and mice treated with PBS are indicated with red lines. The 800 copies ml^{-1} limit of detection of this assay is indicated by a dashed line. Experiments in **a**–**g** were performed at least twice with similar results. Error bars denote s.e.m. of triplicates.

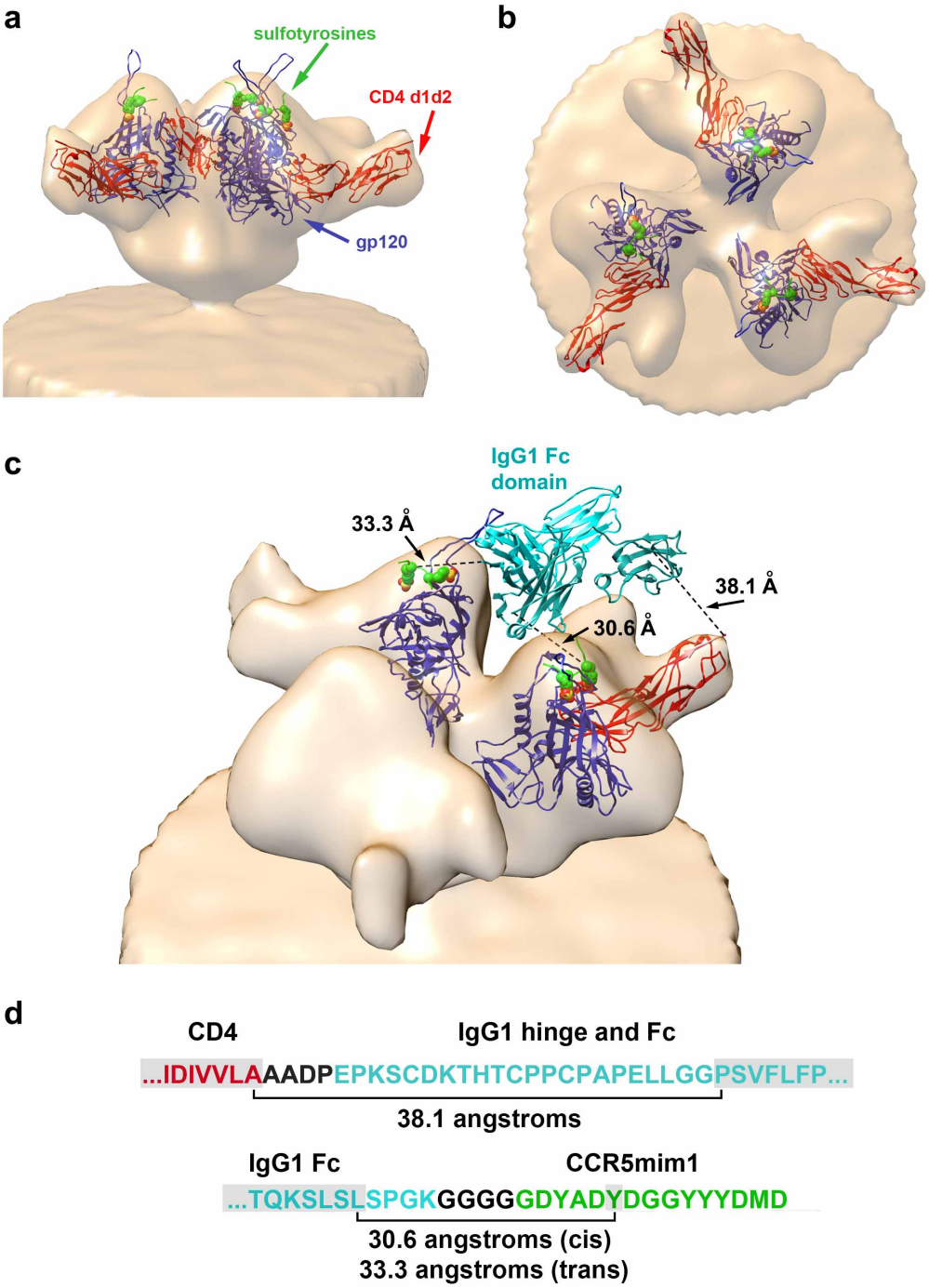

Extended Data Figure 3 | A model of eCD4-Ig bound to the HIV-1 Env trimer. a, The structure (2QAD) of gp120 (YU2 isolate) bound to the tyrosine-sulfated CD4i antibody 412d and CD4 domains 1 and 2 (ref. 10), was fitted into a cryoelectron micrograph of the HIV-1 envelope glycoprotein trimer (Env; Bal isolate) bound to CD4 (ref. 48). gp120 and CD4 domains 1 and 2 are shown in blue and red, respectively. 412d sulfotyrosines are represented as green (carbon), red (oxygen) and yellow (sulphur) spheres. The remainder of 412d was excluded for clarity. **b**, The same structure shown in **a** rotated 90° about the horizontal axis. Note that the sulfotyrosine-binding pockets are proximal to the trimer axis, whereas the C terminus of CD4 domain 2 is distal from the trimer axis, preventing both CD4 domains of CD4-Ig from simultaneously binding the same Env trimer. **c**, A model of how eCD4-Ig may associate with Env is presented. The Fc domain of human IgG1 (1FCC, cyan)[49] was positioned to be proximal to the gp120 sulfopeptide-binding pocket occupied by sulfotyrosine 100 (Tys 100) of the 412d heavy chain while avoiding steric interaction with Env. Tys 100 occupies a pocket in gp120 thought to bind CCR5 sulfotyrosine 10 (ref. 50). This pocket is also critical for binding of CCR5mim1 and CCR5mim 2 (refs 20, 22). In this model, the Fc domain is oriented to allow each eCD4-Ig sulfopeptide to engage a different gp120 protomer[24]. A single CD4 domain also binds one of the sulfopeptide-bound protomers. Distances between the C terminus of CD4 and the N terminus of one Fc domain monomer (38.1 Å), between the C terminus of the Fc domain and Tys 100 pocket of the CD4-bound gp120 protomer (30.6 Å), and between the C terminus of the Fc domain and Tys 100 pocket of an adjacent gp120 protomer (33.3 Å), are indicated. **d**, Residues not visible in the crystal structures used to construct this model are shown between brackets. In the model shown in **c**, these residues span the distances indicated. Note that these distances are well under the extension of a typical beta strand. CD4-, IgG1- and CCR5mim1-derived residues are shown in red, cyan, and green, respectively, with linker regions shown in black. Residues visible in the crystal structures, including the CCR5mim1 sulfotyrosine presumed to fill the Tys 100 pocket, are highlighted in grey. Modelling was performed using UCSF Chimera version 1.8.

a

IC50 values

Virus	Clade	Tier	CD4-Ig	eCD4-Ig	mim2	Q40A	Q40A, mim2	Fold	Geometric Mean: eCD4-Ig variants	Geometric Mean: CD4bs bNAbs
				eCD4-Ig variants						
SF162.LS	B	1A	<0.001	<0.001	<0.001	<0.001	<0.001	1.0	0.001	0.048
BaL.26	B	1B	0.006	<0.001	<0.001	0.001	<0.001	>6	0.001	0.015
DJ263.8	AG	1B	0.018	0.001	0.001	0.004	0.001	12.7	0.001	0.032
ZM109F.PB4	C	1B	0.042	0.002	0.002	0.003	0.002	19.0	0.002	0.063
TV1.21	C	1B	0.045	0.002	0.001	0.008	0.001	22.5	0.002	ND
3365.v2.c20	A	2	0.066	0.002	0.002	0.016	0.002	19.6	0.003	0.020
SIVmac251.30	SIV	3	0.197	0.006	0.007	0.144	0.025	10.0	0.020	>50
QH0692.42	B	2	0.396	0.013	0.013	0.004	0.002	65.3	0.006	0.681
THRO4156.18	B	2	0.508	0.018	0.017	0.009	0.004	49.6	0.010	2.855
Q769.d22	A	2	0.661	0.021	0.028	0.021	0.018	30.4	0.022	0.011
3016.v5.c45	D	2	0.681	0.028	0.029	0.19	0.026	15.2	0.045	0.268
Q259.d2.17	A	2	2.141	0.076	0.079	0.081	0.048	30.8	0.070	0.034
T33-7	AG	3	3.512	0.053	0.053	0.005	0.003	245.1	0.014	0.023
T25118	AG	3	6.071	0.275	0.206	0.125	0.016	58.8	0.103	0.996
AC10.0.29	B	2	6.284	0.179	0.181	0.443	0.331	23.9	0.263	1.466
ZM135M.PL10a	C	2	6.373	0.42	0.272	0.094	0.042	43.7	0.146	0.289
PVO.4	B	3	9.506	0.212	0.214	0.032	0.025	122.5	0.078	0.162
CH115.12	B	3	25.676	0.786	0.554	0.586	0.255	50.8	0.505	ND
Du156.12	C	2	26.267	0.782	0.694	0.173	0.067	93.3	0.282	0.044
T257-31	AG	2	40.001	0.509	0.416	3.429	0.507	51.4	0.779	0.560
X1193_C1	G	2	40.218	0.367	0.476	0.111	0.028	263.5	0.153	ND
TRJO4551.58	B	3	>50	0.717	0.581	0.12	0.052	>221.4	0.226	0.052
TRO.11	B	2	>50	0.917	0.759	0.225	0.131	>132.1	0.378	0.227
R1166.c1	AE	2	>50	1.137	0.983	1.246	0.226	>66.8	0.749	0.890

b

IC50 values

Virus	Clade	CD4-Ig	eCD4-Ig variants: mim2	Q40A, mim2	Fold	NIH 45-46	3BNC117	VRC01
TV1.29	C	0.055	0.001	<0.001	>55.0	>50	>50	>50
Du123.06	C	0.082	<0.001	<0.001	>82.0	>50	0.183	13.6
57128.vrc15	D	0.243	0.007	0.004	45.9	>50	0.432	>50
89-F1_2_25	CD	0.491	0.022	0.008	37.0	>50	>50	ND
CH070.1	BC	0.507	0.010	0.003	92.6	>50	7.89	18.7
CNE7	BC	0.576	0.028	0.005	48.7	0.014	>50	0.54
Du172.17	C	0.821	0.022	0.003	101.1	>50	1.19	>50
Du151.02	C	0.823	0.046	0.011	36.6	>50	>50	7.7
6545.v4.c1	AC	0.835	0.043	0.123	11.5	>50	>50	>50
CAP210.2.00.E8	C	1.033	0.029	0.010	60.7	>50	8.16	>50
ZM247v1(rev-)	C	1.079	0.043	0.056	22.0	2.185	>50	ND
242-14	AG	1.192	0.042	0.006	75.1	>50	>50	>50
X2088.c9	G	1.437	0.075	0.028	31.4	>50	>50	>50
Ce1172_H1	C	1.619	0.127	0.014	38.4	>50	>50	ND
1394C9G1 (rev-)	C	1.738	0.086	0.011	56.5	0.027	>50	ND
T278-50	AG	1.826	0.203	0.665	5.0	>50	>50	>50
CNE15	BC	1.848	0.112	0.006	71.3	0.005	>50	0.08
6540.v4.c1	AC	1.987	0.073	0.192	16.8	>50	>50	>50
6322.v4.c1	C	2.282	0.100	0.029	42.4	>50	>50	>50
6631.v3.c10	C	2.396	0.102	0.197	16.9	>50	>50	>50
7165.18	B	2.469	0.143	0.038	33.5	>50	6.54	>50
CNE20	BC	2.583	0.123	0.050	32.9	3.682	>50	ND
6471.v1.c16	C	2.662	0.164	0.036	34.6	>50	>50	>50
CH038.12	BC	3.490	0.139	0.176	22.3	0.059	>50	0.379
00836-2.5	C	3.566	0.093	0.025	74.0	<0.001	>50	0.128
A03349M1.vrc4a	D	3.874	0.176	0.018	68.8	>50	0.512	4.66
6545.v3.c13	AC	3.960	0.092	0.501	18.4	>50	>50	ND
Du422.1	C	4.268	0.157	0.036	56.8	>50	>50	>50
H086.8	B	6.522	0.071	0.088	82.5	>50	>50	>50
T251-18	AG	7.626	0.188	0.035	94.0	0.863	0.203	3.58
CAP45.2.00.G3	C	7.661	0.140	0.029	120.2	>50	0.589	9.47
T250-4	AG	8.961	0.218	0.006	247.8	>50	>50	>50
T266-60	AG	10.982	0.377	0.029	105.0	0.363	0.032	0.353
0077.V1.C16	C	12.703	0.245	0.042	125.2	0.160	>50	1.04
3718.v3.c11	A	15.392	0.676	0.401	29.6	2.049	>50	0.218
191955_A11	A	20.979	0.454	0.757	35.8	0.116	>50	ND
3988.25	B	21.728	0.623	1.332	23.9	0.071	>50	2.1
3637.v5.c3	C	28.616	0.655	0.046	164.9	0.799	>50	4.09
3817.v2.c59	CD	30.770	1.453	0.130	70.8	>50	0.216	>50
620345.c1	AE	46.395	0.515	0.051	286.3	>50	>50	>50

μg/ml	<0.01	0.01-0.1	0.1-1	1 to 10	10 to 50	>50	NOT DONE
nM	<0.1	0.1 to 1	1 to 10	10 to 100	100-500	>500	

Extended Data Figure 4 | IC_{50} values of eCD4-Ig variants against neutralization-resistant isolates. **a**, The IC_{50} values (μg ml^{-1}) of CD4-Ig, eCD4-Ig, eCD4-Ig^{mim2} (mim2), eCD4-Ig^{Q40A} (Q40A) and eCD4-Ig^{Q40A,mim2} (Q40A,mim2) against 24 HIV-1 and SIV isolates selected for their neutralization resistance are shown. The clade and tier of each isolate is listed. HIV-1 pseudotyped with the indicated envelope glycoprotein was incubated in triplicate with TZM-bl cells and varying concentrations of CD4-Ig or eCD4-Ig variant. Luciferase activity was determined 2 days after infection. 'Fold' indicates the ratio of the IC_{50} value of CD4-Ig to the geometric mean of the IC_{50} values of the assayed eCD4-Ig variants. The geometric mean of eCD4-Ig variants and the CD4bs antibodies 3BCN117, NIH45-46 and VRC01 calculated from values reported in previously[4,6] are shown in the two right-most columns. **b**, Neutralization studies similar to those in **a** except that the IC_{50} values of CD4-Ig, eCD4-Ig^{mim2} (mim2), eCD4-Ig^{Q40A,mim2} (Q40A,mim2) and NIH45-46 were determined for a panel of 40 viral isolates selected for their resistance to the CD4bs bNAbs 3BNC117 and NIH45-46. IC_{50} values of the CD4bs antibodies VRC01 and 3BNC117 listed in the two right-most columns were previously reported[4,6].

a

IC80 values — eCD4-Ig variants

Virus	Clade	Tier	CD4-Ig	eCD4-Ig	mim2	Q40A	Q40A, mim2	Fold	Geometric Mean: eCD4-Ig variants	Geometric Mean: CD4bs bNAbs	NIH45-46	3BNC117	VRC01
SF162.LS	B	1A	<0.001	<0.001	<0.001	<0.001	<0.001	1.0	<0.001	0.181	0.113	0.084	0.627
BaL.26	B	1B	0.041	0.002	0.002	0.002	0.001	24.4	0.002	0.061	0.052	0.028	0.154
DJ263.8	AG	1B	0.12	0.004	0.005	0.023	0.003	19.7	0.006	0.212	0.108	0.133	0.668
ZM109F.PB4	C	1B	0.316	0.014	0.014	0.045	0.025	14.6	0.022	0.329	0.373	0.242	0.394
TV1.21	C	1B	0.211	0.006	0.005	0.028	0.003	29.8	0.007	ND	ND	ND	ND
3365.v2.c20	A	2	0.294	0.016	0.015	0.101	0.012	12.7	0.023	0.090	0.185	0.044	ND
SIVmac251.30	SIV	3	1.443	0.191	0.148	5.605	0.841	2.4	0.604	>50	>50	>50	>50
QH0692.42	B	2	2.756	0.102	0.066	0.017	0.011	82.3	0.033	2.463	3.39	1.47	3
THRO4156.18	B	2	1.858	0.068	0.065	0.025	0.019	48.8	0.038	12.569	9.67	13.6	15.1
Q769.d22	A	2	7.248	0.119	0.155	0.116	0.097	60.4	0.120	0.067	0.09	0.045	0.074
3016.v5.c45	D	2	3.496	0.108	0.108	0.989	0.139	17.5	0.200	1.069	>50	3.35	0.341
Q259.d2.17	A	2	11.764	0.373	0.283	0.367	0.245	37.7	0.312	0.145	0.181	0.067	0.252
T33-7	AG	3	22.853	0.282	0.204	0.027	0.016	323.7	0.071	0.057	0.392	0.021	0.023
T25118	AG	3	40.544	1.259	0.743	0.578	0.064	94.0	0.431	4.783	12.5	0.858	10.2
AC10.0.29	B	2	35.017	0.693	0.535	1.691	1.608	34.9	1.002	2.916	2.22	>50	3.83
ZM135M.PL10a	C	2	45.557	1.677	0.83	0.526	0.433	60.7	0.750	1.708	2.89	0.28	6.16
PVO.4	B	3	>50	1.491	0.982	0.152	0.145	>118.0	0.424	0.517	0.474	0.294	0.99
CH115.12	B	3	>50	2.798	1.591	2.113	0.792	>30.3	1.652	ND	ND	ND	ND
Du156.12	C	2	>50	3.873	3.391	0.858	0.513	>32.2	1.551	0.127	0.07	0.121	0.244
T257-31	AG	2	>50	1.404	1.161	10.363	1.817	>21.2	2.354	2.047	2.13	0.694	5.8
X1193_C1	G	2	>50	2.364	2.092	0.66	0.119	>63.3	0.789	ND	ND	ND	ND
TRJO4551.58	B	3	>50	2.518	1.658	0.346	0.251	>64.4	0.776	0.179	0.111	0.216	0.239
TRO.11	B	2	>50	4.494	2.745	1.609	0.665	>26.2	1.906	0.955	6.4	0.125	1.09
R1166.c1	AE	2	>50	6.176	3.843	6.36	0.869	>14.8	3.384	3.415	7.02	0.805	7.05

b

IC80 values — eCD4-Ig variants:

Virus	Clade	CD4-Ig	mim2	Q40A, mim2	Fold	NIH 45-46	3BNC117	VRC01
TV1.29	C	0.196	0.005	0.003	50.6	>50	>50	>50
Du123.06	C	0.437	0.016	0.004	54.6	>50	1.17	>50
57128.vrc15	D	1.057	0.045	0.013	43.7	>50	1.84	>50
89-F1_2_25	CD	2.077	0.056	0.018	65.4	>50	>50	ND
CH070.1	BC	1.811	0.039	0.013	80.4	>50	50	50
CNE7	BC	2.861	0.111	0.017	65.9	0.085	>50	1.36
Du172.17	C	5.645	0.151	0.020	102.7	>50	2.46	>50
Du151.02	C	3.891	0.168	0.028	56.7	>50	>50	>50
6545.v4.c1	AC	5.089	0.182	0.483	17.2	>50	>50	>50
CAP210.2.00.E8	C	7.958	0.180	0.041	92.6	>50	>50	>50
ZM247v1(rev-)	C	5.702	0.189	0.245	26.5	>50	>50	ND
242-14	AG	18.026	0.378	0.052	128.6	>50	>50	>50
X2088.c9	G	5.026	0.252	0.082	35.0	>50	>50	>50
Ce1172_H1	C	13.312	0.460	0.062	78.8	>50	>50	ND
1394C9G1 (rev-)	C	39.283	0.732	0.082	160.3	0.161	>50	ND
T278-50	AG	14.186	0.971	3.419	7.8	>50	>50	>50
CNE15	BC	22.835	0.461	0.023	221.8	0.018	>50	0.28
6540.v4.c1	AC	17.253	0.337	1.338	25.7	>50	>50	>50
6322.v4.c1	C	10.366	0.425	0.121	45.7	>50	>50	>50
6631.v3.c10	C	7.926	0.233	0.666	20.1	>50	>50	>50
7165.18	B	12.997	0.558	0.172	42.0	>50	35.7	>50
CNE20	BC	23.876	0.719	0.346	47.9	>50	>50	ND
6471.v1.c16	C	13.816	0.623	0.137	47.3	>50	>50	>50
CH038.12	BC	19.888	0.527	0.937	28.3	0.221	>50	1.53
00836-2.5	C	38.764	0.744	0.138	121.0	0.007	>50	0.52
A03349M1.vrc4a	D	17.546	0.468	0.054	110.4	>50	2.34	28.1
6545.v3.c13	AC	15.344	0.442	1.748	17.5	>50	>50	ND
Du422.1	C	27.666	1.463	0.161	57.0	>50	>50	>50
H086.8	B	26.707	0.491	1.153	35.5	>50	>50	>50
T251-18	AG	41.025	0.509	0.102	180.0	3.134	0.858	10.2
CAP45.2.00.G3	C	41.712	0.714	0.120	142.5	>50	32.1	>50
T250-4	AG	33.879	0.769	0.032	216.0	>50	>50	>50
T266-60	AG	>50	1.503	0.159	>102.3	2.379	0.119	1.35
0077.V1.C16	C	>50	1.816	0.235	>76.5	0.767	>50	3.65
3718.v3.c11	A	>50	1.841	0.952	>37.8	>50	>50	4.99
191955_A11	A	>50	1.556	2.630	>24.7	0.592	>50	ND
3988.25	B	>50	2.288	11.626	>9.7	0.353	>50	>50
3637.v5.c3	C	>50	1.509	0.128	>113.8	3.069	>50	11.0
3817.v2.c59	CD	>50	5.133	0.366	>36.5	>50	0.752	>50
620345.c1	AE	>50	2.876	0.201	>65.8	>50	>50	>50

μg/ml	<0.01	0.01-0.1	0.1-1	1 to 10	10 to 50	>50	NOT DONE
nM	<0.1	0.1 to 1	1 to 10	10 to 100	100-500	>500	

Extended Data Figure 5 | IC_{80} values of eCD4-Ig variants against neutralization-resistant isolates. **a**, **b**, The IC_{80} values ($\mu g\,ml^{-1}$) of the experiments described in Extended Data Fig. 5a (**a**) and Extended Data Fig. 5b (**b**) are shown.

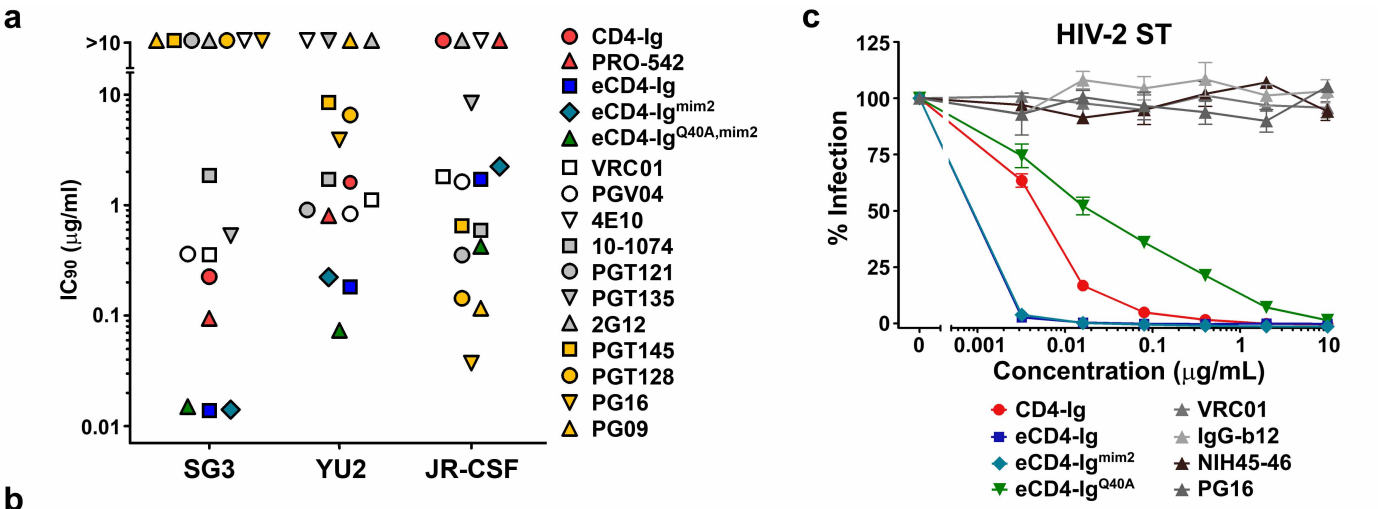

b

IC_{50} values

Virus	CD4-Ig	eCD4-Ig variants: eCD4-Ig	mim2	Q40A, mim2	VRC01	VRC-PG04	PGT145	PG09	PG16	4E10	2G12	PGT121	PGT128	PGT135	10-1074	PRO542
SG3	0.027	0.002	0.002	0.003	0.060	0.060	> 10	> 10	> 10	1.540	0.981	0.121	> 10	0.076	0.154	0.012
+/-	0.002	0.000	0.000	0.001	0.009	0.014	0.000	0.000	0.000	0.499	0.153	0.023	0.000	0.020	0.021	0.002
YU2	0.293	0.030	0.035	0.015	0.134	0.116	1.842	3.702	0.145	> 10	> 10	0.121	0.244	> 10	0.280	0.115
+/-	0.043	0.003	0.004	0.000	0.005	0.002	0.279	0.481	0.009	0.000	0.000	0.021	0.059	0.000	0.028	0.014
JR-CSF	3.175	0.237	0.270	0.064	0.285	0.188	0.052	0.013	0.004	3.103	0.995	0.055	0.020	0.859	0.097	1.588
+/-	0.635	0.023	0.043	0.006	0.074	0.061	0.004	0.002	0.000	0.120	0.096	0.020	0.008	0.066	0.014	0.115

IC_{90} values

Virus	CD4-Ig	eCD4-Ig variants: eCD4-Ig	mim2	Q40A, mim2	VRC01	VRC-PG04	PGT145	PG09	PG16	4E10	2G12	PGT121	PGT128	PGT135	10-1074	PRO542
SG3	0.225	0.014	0.014	0.015	0.356	0.360	> 10	> 10	> 10	> 10	> 10	> 10	> 10	0.529	1.860	0.094
+/-	0.023	0.001	0.000	0.001	0.018	0.031	> 10	0.000	0.000	0.000	0.000	0.000	0.000	0.178	0.012	0.013
YU2	1.607	0.182	0.223	0.074	1.113	0.836	8.519	> 10	3.896	> 10	> 10	0.906	6.544	> 10	1.717	0.802
+/-	0.040	0.013	0.017	0.001	0.012	0.030	0.992	0.000	1.341	0.000	0.000	0.157	1.125	0.000	0.074	0.096
JR-CSF	> 10	1.709	2.237	0.423	1.812	1.629	0.651	0.117	0.037	> 10	> 10	0.353	0.144	8.429	0.593	> 10
+/-	0.000	0.087	0.401	0.077	0.134	0.255	0.303	0.006	0.005	0.000	0.000	0.038	0.042	0.137	0.096	0.000

Extended Data Figure 6 | Further comparison of eCD4-Ig and HIV-1 neutralizing antibodies. **a**, IC_{90} values for the same experiments shown in Fig. 2a, presented in the same format. **b**, Numeric IC_{50} and IC_{90} values of the experiment shown in **a** and Fig. 2a are shown, using the same colour coding of Extended Data Figs 4 and 5. The s.e.m. of triplicates are indicated below their IC_{50} and IC_{90} values. **c**, Experiments similar to those in Fig. 2b except that HIV-1 pseudotyped with the Env of the HIV-2 isolate ST was incubated with the indicated concentrations of CD4-Ig, eCD4-Ig variants or the CD4bs antibodies IgG-b12, VRC01 or NIH45-46. Error bars denote s.e.m. of triplicates.

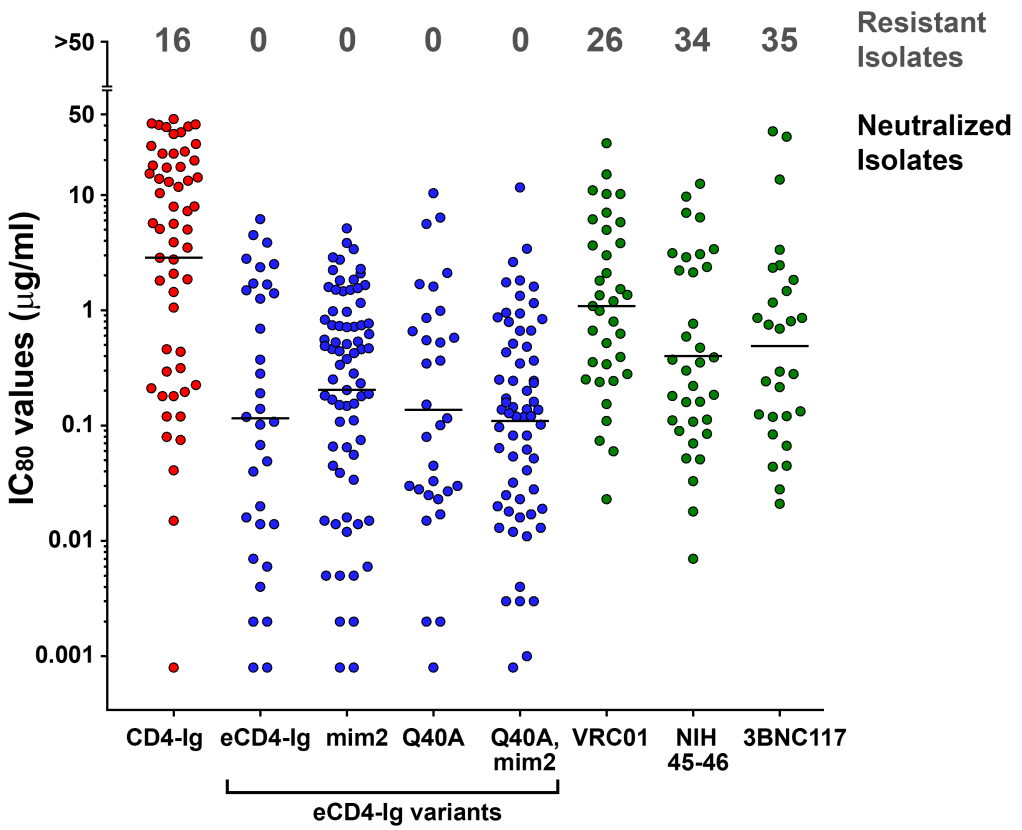

Extended Data Figure 7 | Summary of IC_{80} values for HIV-1, HIV-2 and SIV neutralization studies. The IC_{80} values from studies of Figs 1b, 2a, b, and Extended Data Figs 4–6 are plotted. The number of isolates resistant to 50 μg ml^{-1} of the indicated inhibitors are indicated at the top. Geometric means are calculated for neutralized isolates and indicated with horizontal lines.

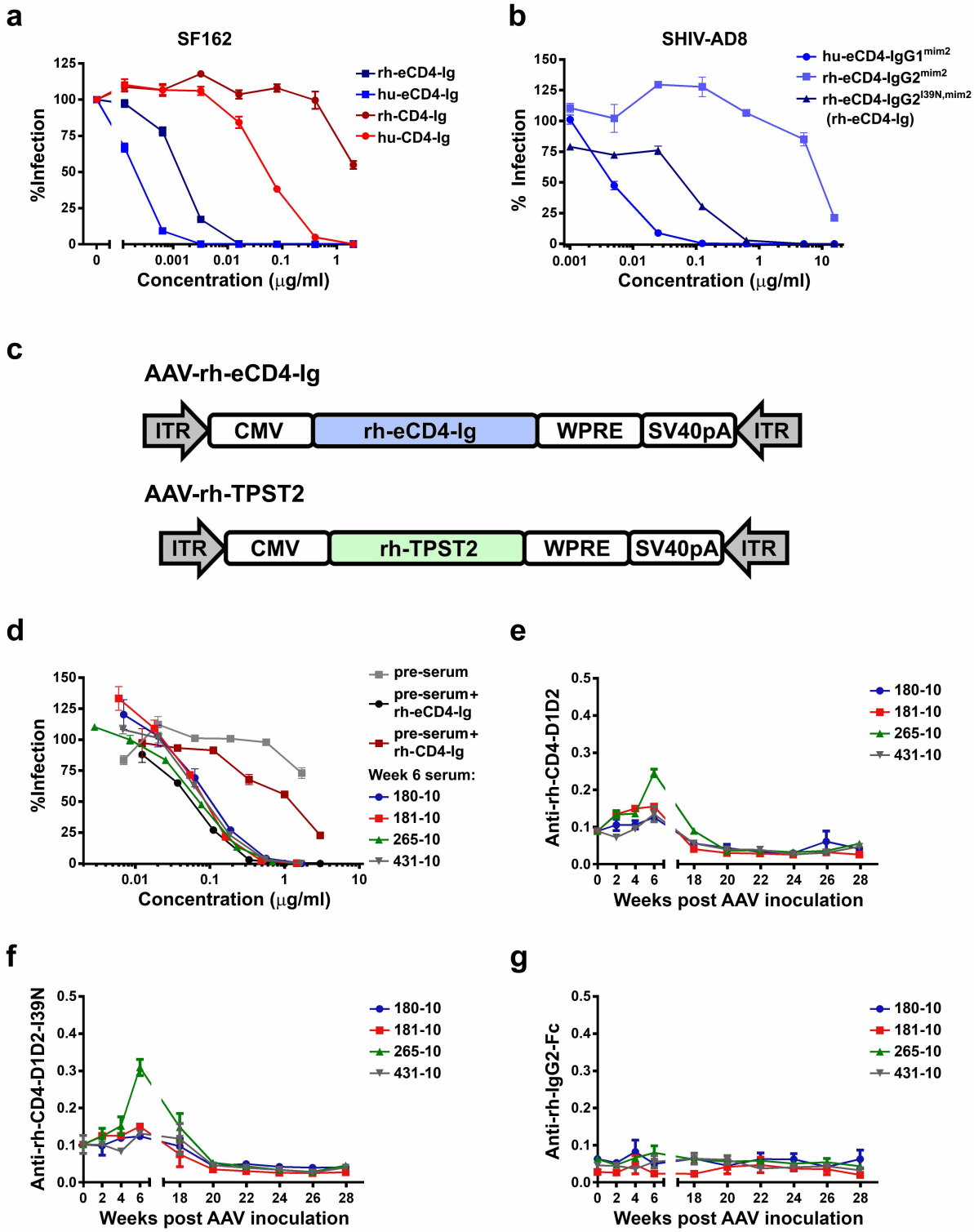

Extended Data Figure 8 | Additional characterization of rh-eCD4-Ig. **a**, An experiment similar to that in Fig. 2b, except that rhesus and human CD4-Ig and eCD4-Ig are compared for their ability to neutralize HIV-1 pseudotyped with the SF162 envelope glycoprotein. All variants have wild-type rhesus or human CD4 domains. Note that variants bearing rhesus CD4 are markedly less potent at neutralizing HIV-1. **b**, Experiment similar to **a** and Fig. 2b except that human eCD4-Ig^{mim2} and its rhesus analogue bearing or not bearing the Ile39Asn mutation are compared using SHIV-AD8. Note that the Ile39Asn mutation largely restores the neutralization activity of rhesus eCD4-Ig^{mim2}. **c**, A representation of the AAV vectors used in the non-human primate studies of Fig. 4. Rh-eCD4-Ig (rh-eCD4-IgG2^{I39N,mim2}; blue) and rhesus tyrosine protein sulfotransferase 2 (TPST2; green) were introduced into a single-stranded AAV vector downstream of a CMV promoter. A woodchuck response element (WPRE), used to promote expression, and the SV40 polyadenylation signal (SV40pA) were also included. AAV inverted terminal repeats (ITR) are indicated in grey arrows. **d**, An experiment similar to that in Fig. 4d except that sera from week 6 were analysed. **e**–**g**, Experiments similar to those in Fig. 4f–h except that the reactivity of rhesus sera was examined for a construct bearing wild-type rhesus CD4 domains 1 and 2 fused to the human IgG1 Fc domain (**e**), one bearing rhesus CD4 domains 1 and 2 with the Ile39Asn mutation, again fused to the human IgG1 Fc domain (**f**), or the antibody NIH45-46 fused to the rhesus IgG2 constant regions, used here to present the rhesus IgG2 Fc domain (**g**). Experiments in **a**, **b** and **d**–**g** represent at least two with similar results. Error bars denote s.e.m. of triplicates.

Extended Data Table 1 | Potencies and breadth of well-characterized broadly neutralizing antibodies

Antibody	IC_{50}	IC_{80}	IC_{50} < 50 μg/ml	IC_{80} < 5 μg/ml
10-1074	0.053	0.217	57.8%	51.2%
35O22	0.057	n.a.	61.9%	n.a. (<61.9%)
PGT121	0.060	0.274	63.0%	47.9%
PGT128	0.069	n.a.	62.9%	n.a. (<62.9%)
PG16	0.092	0.178	55.6%	43.6%
3BNC117	0.111	0.345	82.2%	61.0%
VRC07	0.114	0.187	83.2%	86.0%
NIH45-46	0.139	0.540	83.7%	57.4%
12A12	0.171	1.101	93.2%	68.9%
PG9	0.176	0.427	77.3%	62.0%
10E8	0.262	1.536	98.3%	75.5%
VRC01	0.306	0.913	88.0%	69.7%

A summary of antibody neutralization potencies compiled using the Los Alamos National Laboratory Database CATNAP tool (http://www.hiv.lanl.gov/components/sequence/HIV/neutralization/main.comp). The geometric mean IC_{50} and IC_{80} values are listed for the indicated bNAbs against all reported isolates, excluding those with values greater than 50 μg ml^{-1}. The percentage of isolates neutralized with IC_{50} values less than 50 μg ml^{-1}, or with IC_{80} values less than 5 μg ml^{-1} are shown. bNAbs are ranked by their geometric mean IC_{50} values. See Fig. 3 and Extended Data Fig. 7 for comparisons of eCD4-Ig variants with the bNAbs NIH45-46, 3BNC117 and VRC01.